Presence, Bioconcentration and Fate of Galaxolide and Tonalide Fragrances in the North Saskatchewan River, Edmonton

Claudine Lefebvre

Thesis submitted to the

Faculty of Graduate and Postdoctoral Studies

in partial fulfillment of the requirements for the

Masters of Science, Biology

Specialization in Chemical and Environmental Toxicology

Ottawa-Carleton Institute for Biology

and

Faculty of Science, University of Ottawa

Thèse soumise à la

Faculté des études supérieures et postdoctorales

dans le cadre des exigences du programme de

Maîtrise ès Sciences, Biologie

Spécialisation en Toxicologie Chimique et Environnementale

Institut de Biologie Ottawa-Carleton

et

Faculté des sciences, Université d'Ottawa

Abstract

Synthetic musks are incorporated extensively in personal care products to improve their scent, increase their fragrance stability, and prolong their shelf-life. As a consequence, these persistent musks are being released at a considerable rate by wastewater treatment plants and are frequently detected in surface water, bottom sediment, air, and aquatic biota near urban areas. In addition to their hydrophobicity, two synthetic musks, Galaxolide (HHCB) and Tonalide (AHTN), were reported to cause endocrine disruption in fish species. Although most of the toxic effects in past studies were observed at high doses, HHCB and AHTN were shown to bioaccumulate very differently depending on the aquatic species tested. As bioaccumulation and fate of contaminants are important considerations when regulating persistent chemicals, an improved understanding of the bioaccumulation potential of these chemicals is needed. In this thesis, an assessment of the presence, bioconcentration and fate of HHCB and AHTH was provided in an area exposed to the effluent of the Gold Bar wastewater treatment plant in the North Saskatchewan River (Edmonton). HHCB and AHTN were quantified in fathead minnows (*Pimephales promelas*) exposed downstream of the effluent, with an adapted method for analysis of musks in fish, using PAHs as recovery standards. Method development and recoveries are summarized. Highest bioconcentration factors were 24,500 and 22,300 for HHCB and AHTN respectively, and were observed 1 km downstream of the outfall. Musks were found in most fathead minnows exposed at reference sites upstream as well as at the furthest site, 9.9 km from the outfall. Musk concentrations in water at these sites were used in the assessment of the fate of HHCB and AHTN by fugacity modeling with QWASI software. In order to assess fate, a contaminated portion of the North Saskatchewan River was divided in a series of compartments that were each treated as connected individual water bodies. HHCB and AHTN losses were mostly due to water advection and sedimentation fluxes. Model fit was assessed by comparing predicted to measured data.

Résumé

Les muscs synthétiques sont incorporés dans une grande variété de produits de beauté dans le but de donner une stabilité à leur fragrance et ainsi prolonger leur durée de vie. En conséquence, ces muscs persistants sont déversés de façon considérable par les usines d'épurations des eaux usées et ont été détectés dans les plans d'eau urbain, les sédiments, l'air et certaines espèces aquatiques. En plus de perturber le système endocrinien, les muscs synthétiques Galaxolide (HHCB) et Tonalide (AHTN) possèdent des propriétés hydrophobiques permettant la bioaccumulation dans les tissues des biotes. Bien que HHCB et AHTN ne causent des effets qu'à des doses relativement élevées, la variation intrinsèque des facteurs de bioaccumulation et bioconcentration publiés par des études antérieures montrent que les dynamiques d'accumulation varient grandement selon l'espèce. La bioaccumulation des contaminants persistants et leur destin sont des indicateurs important dans la prise de décisions sur leur régulation. Ce mémoire a apporté une évaluation du degré de contamination, de bioconcentration et du destin de HHCB et AHTN lorsque déversés dans la Rivière Saskatchewan Nord par les installations de traitement des eaux usées Gold Bar (Edmonton). Pour ce faire, HHCB et AHTN ont été quantifiés dans des menés (*Pimephales promelas*) exposés en amont et en aval de l'effluent, avec une méthode d'analyse utilisant des HAPs deutérés comme étalon interne. Cette méthode ainsi que ces taux de recouvrement ont été rapportés. Les facteurs de bioconcentration les plus élevés, 24 500 pour HHCB et 22 300 pour AHTN, ont été trouvés dans les menés exposés à 1 km en aval du point d'émission. Des muscs ont été décelés dans les poissons exposés aux sites de référence en amont de la source d'émission, ainsi qu'au site le plus loin en aval (9.9 km). Les concentrations de HHCB et AHTN dans l'eau de la Rivière Saskatchewan Nord ont été utilisées dans la détermination de leur destin par modélisation de la fugacité avec le programme QWASI. La portion contaminée de la rivière a été divisée en une série de compartiments traités individuellement comme une série de plans d'eau connectés. Les pertes de HHCB et AHTN ont été principalement par advection de l'eau et par sédimentation. La validité et la capacité d'adaptation du modèle aux concentrations mesurées dans l'eau ont été évaluées.

Acknowledgements

Firstly, I would like to thank Dr. Jules M. Blais and Dr. Vance L. Trudeau for their wonderfully warm welcome in the Chemical and Environmental Toxicology program. This project would not have been possible without their professional insight, advice and financial support, which were greatly appreciated through all the steps of this project. Also, a special thank you for their patience toward my English writing skills. I am very grateful to Linda E. Kimpe for providing training with laboratory equipment and methods as well as sharing her expertise with me during the first part of my project. Thank you for making the laboratory one of the best environment I worked in.

I am thankful to my thesis committee Dr. Thomas W. Moon and Dr. Robert Letcher for their guidance, as well as Dr. Chris Metcalfe from Trent University for contributing to the data presented in this thesis. I would like to thank our colleagues from the University of Alberta who organized and conducted field exposures as well as the Canadian Water Network for funding this project.

I want to give a special mention to former graduate students David Eickmeyer, Rebecca D'Onofrio and Adam Houben for trusting me with their lab work when I was a starting as an assistant, who gave me the opportunity to acquire useful experience. As a graduate student now, it is my turn to acknowledge the assistance of Tri-An Nguyen, Nicholas Kim, Krishna Gelda and Lauren Gallant during my lab work. To all my lab mates, with whom I shared fun moments inside and outside the lab, thank you for your continuous moral support throughout this project. I am grateful to my family for being understanding during this time as well as their moral and financial support, especially during the very last stretch. Finally, a special thank you to two of my very close friends and accomplished women scientists, Élysabeth Théberge and Martine Cordeau, for inspiring me to work harder. Thank you for the breaks we shared together and the fun phone conversations that I continue to treasure to this day.

Sincerely,

Claudine Lefebvre

Gatineau, September 2015

Table of contents

List of Tables

List of Figures

List of Abbreviations

ACRWWTP	Alberta capital region wastewater treatment plant
AESRD	Alberta environment and sustainable resource development
AHTN	7-acetyl-1,1,3,4,4,6-hexamethyltetrahydronaphtalene
ANOVA	Analysis of variance
ASE	Accelerated solvent extractor
BAF	Bioaccumulation factor
BCF	Bioconcentration factor
BFC	Benzo-4-trifluoromethyl-coumarin
CAT	Catalase
CSO	Combined sewer outfall
DCM	Dichloromethane
EA	Ethyl acetate
EDCs	Endocrine disruptive chemicals
EPA	Environmental protection agency
ERα - ERβ	Estrogen receptor α or β
E2	17β-estradiol
FHM(s)	Fathead minnow(s)
GBWWTP	Gold Bar wastewater treatment plant
GC-MSD	Gas chromatograph – mass selective detector
GPC	Gel permeation chromatography
GSSG	Oxidized glutathione
IC50	Half-maximal inhibitory concentration
IH-CR	Industrial heartland – capital region
HERA	Human and environmental risk assessment on ingredients of household cleaning products
hERα	Human estrogen receptor α
HEX	n-Hexanes
HHCB	1,3,4,6,7,8-hexahydro-4,6,6,7,8,8-hexamethylcyclopenta(g)-2-benzopyrane
HPLC	High performance liquid chromatography
KOH	Potassium hydroxide
K_{OW}	Octanol-water partition coefficient
LOEC	Lowest observed effect concentration
MDA	Malondialdehyde
MS-222	Tricaine methanesulfonate
NSR	North Saskatchewan River
OSPAR	Oslo-Paris commission for protection and conservation of the North-East Atlantic and its resources
PAH	Polycyclic aromatic hydrocarbon
PBO	Piperonyl butoxide
PCB	Polychlorinated biphenyls
POD	Peroxidase
POP	Persistent organic pollutant
PR	Progesterone receptor
PTFE	Polytetrafluoroethylene
QWASI	Quantitative water air sediment interaction
RSD	Relative standard deviation
SE	Standard error
SERM	Selective estrogen receptor modulator

SOD	Superoxide dismutase
SPE	Solid phase extraction
SPMD	Semi-permeable membrane device
STP	Sewage treatment plant
TGSH	Total glutathione
TMP	2,2,4-trimethylpentane
UV	Ultraviolet
VTG	Vitellogenin
ww	Wet weight
WTP	Water treatment plant
WWTP	Wastewater treatment plant
YES	Yeast estrogenic assay

Thesis objectives

The polycyclic musks 1,3,4,6,7,8-hexahydro-4,6,6,7,8,8-hexamethylcyclopenta(g)-2-benzopyrane (HHCB, or Galaxolide) and 7-acetyl-1,1,3,4,4,6-hexamethyltetrahydronaphtalene (AHTN, or Tonalide) are currently among the most abundant personal care product contaminants released by wastewater treatment plant effluents (Del Río et al., 2013; Santiago-Morales et al., 2013). Public concern is growing on their presence in urban waters as well as their potential as endocrine disrupting chemicals (Simmons et al., 2010; Schreurs et al., 2002; Van der Burg et al., 2008). The main objective of this thesis is to document the biological accumulation and distribution of these contaminants in an urban river exposed to the effluents from a growing human population, in order to provide information for risk and exposure assessments. As they were introduced relatively recently, research is still needed to properly assess the potential threat that musks pose to the environment. The three following objectives were identified in order to assess the environmental risks associated with these musks in urban waterbodies.

Objective #1. To optimize an efficient laboratory procedure for quantitation of the polycyclic musks HHCB and AHTN with polycyclic aromatic hydrocarbons (PAHs) as standards in a fish tissue matrix.

Objective #2. To assess the presence and bioconcentration of polycyclic musks HHCB and AHTN in caged fathead minnows exposed to the effluents of Gold Bar sewage treatment plant in the North Saskatchewan River, Edmonton (Alberta, CAN).

Objective #3. To determine the partitioning and fate of HHCB and AHTN fragrances in the North Saskatchewan River using fugacity-based modeling coupled with field collected data.

Chapter 1

1. Introduction

1.1 History and general information concerning musk chemicals

In the early 1900s, musk fragrances muscone and civetone (macrocyclic musks) were collected and extracted from animals like the male musk deer (*Moschus moschiferus L.*) found in China, Tibet and Siberia, and African and Asian civet cats (*Viverra civetta* and *Viverra zibetha*). The harvest of such musks required sacrifice of the animal. With time and development, cheaper sources of natural musks were exploited from muskrat (*Ondatra zibethica*) to angelica roots (*Archangelica officinalis*). Furthermore, in 1979, the Convention on International Trade in Endangered Species of Wild Fauna and Flora, plus complimentary additional laws, restricted the hunting of musk deer (Franke et al., 1999). As a result, alkylnitrobenzenes compounds (synthetic nitro musks) were discovered to possess musky scents, and two of those, musk xylene and musk ketone, started to be widely used in the perfume industry. Fragrances possessing a macrocyclic structure were investigated as well and synthesized but failed economically against the simple and cost-effective production of nitro musks (Rowe, 2005).

Nitro musks and their degradation products, which are benzene rings with methyl, nitrate, acetyl and tert-butyl functional groups, proved to be toxic. For example, musk ambrette showed neurotoxicity (Spencer et al., 1984) and induced growth retardation and progressive paralysis of the hind limbs in rats (Davis et al., 1967). Musk xylol was carcinogenic in rats (Maekawa et al., 1990). Restrictions were then applied in Europe (OSPAR, 2004; ECHA, 2012), and accordingly, their presence radically decreased in personal care products as well as in the environment, as they were replaced by polycyclic musks as an alternative (Lung et al., 2011; Zhang et al., 2008).

In the 1970s, polycyclic musk production and usage bloomed, and they are currently used globally in personal care products and household cleaning products, such as deodorants, shampoos, cosmetics, skin creams, soaps, detergents, and fabric softeners. In addition to their scents, polycyclic musks act as fixatives

because of their stability; they help maintain the integrity of the commercial product for long periods and extend shelf life. They are the basic ingredient in most of the marketed scents.

Among the polycyclic musk family, 1,3,4,6,7,8-hexahydro-4,6,6,7,8,8-hexamethylcyclopenta(g)-2-benzopyrane (HHCB, or Galaxolide) and 7-acetyl-1,1,3,4,4,6-hexamethyltetrahydronaphtalene (AHTN, or Tonalide) are the two most important : they represented 95% of all polycyclic musks used in the European Union market and 90% of the United-States market in 2004 (HERA, 2004). Their production and marketing is closely monitored, in Europe, by the Oslo-Paris Commission for Protection and Conservation of the North-East Atlantic and its resources (OSPAR) since 2003. This project focused on HHCB and AHTN due to their high production and large market share in the musk industry, and due to their hydrophobic, bioaccumulative and toxic properties, which will be reviewed in the following sections.

1.2. Causes of musks contamination in the environment

Synthetic musks are released in rivers and lakes mostly by effluents from sewage treatment plants (STP). The wastewater produced by industrial and human activities, such as cleaning and showering, contains typically several $\mu g \cdot L^{-1}$ of musks, and is generally depending on the population size (Bester, 2005; Clara et al., 2011). The STP influents are cleaned by sedimentation and aeration that remove a substantial fraction of contaminants. Elimination efficiency in most STP effluents vary between 40 and 100% around the world, according to data from 33 STPs in Germany, Switzerland, UK, USA and The Netherlands (HERA, 2004). The removal of HHCB and AHTN in three different STPs in Germany was assessed by Bester (2005). The elimination rates at STP A, B and Dortmund[1] along the Ruhr River were respectively 78%, 83% and 63% for HHCB, and 76%, 87% and 64% for AHTN, which represented a discharge of hundreds of nanograms of fragrance per litre of effluent. In Toronto, total concentrations of HHCB and AHTN were up to 1,000 $ng \cdot L^{-1}$ in water sampled in various rivers and creek surrounding the city, and up to 5,400 $ng \cdot L^{-1}$ in WWTP effluents (Melymuk et al., 2014). In addition to WWTP effluents, the leaching

[1] The identity of the STPs where the elimination rates were calculated is not specified. Arbitrary names were given (A, B and Dortmund, the latter being the name of the city where the STP is located).

process occurring at landfill sites is also considered a source of musks in the environment (Sumner et al., 2010).

1.3. Presence of musks in urban areas

HHCB and AHTN were found in several environmental compartments in urban areas. In outdoor air from urban and rural areas of Iowa and the Great Lakes, levels found varied between 1 and 5 $ng \cdot m^{-3}$, and were comparable or greater than gas-phase pesticide concentrations in rural areas (Peck et al., 2006;). In indoor air from Berlin, HHCB and AHTN median values were 101 and 44 $ng \cdot m^{-3}$ (Fromme et al., 2004). Dust collected and analysed in the same study showed median values of 0.7 and 0.9 $mg \cdot kg^{-1}$ of dust, respectively. Surface waters and sediment from Suzhou Creek, a river passing through Shanghai (China), contained musks. In surface water, HHCB and AHTN concentrations were 20-93 $ng \cdot L^{-1}$ and 8-20 $ng \cdot L^{-1}$, and in sediment, 3-78 $ng \cdot g^{-1}$ and 2-31 $ng \cdot g^{-1}$ (Zhang et al., 2008). Levels reported in biota and in fish varied widely, between 20 to 3,500 $ng \cdot g^{-1}$ (wet weight total musks) depending on the species and the location (O'Toole et al., 2006; Hu et al., 2011; Gatermann et al., 2002). Musks also have been detected and quantified in breast milk samples from Germany (Rimkus et al., 1994) and human blood samples from China (Hu et al., 2009).

1.4. Physicochemical properties

The structures of the two most common musks in this family (Figure 1.1) consist mostly of non-polar functional groups. For both musks, partition coefficients (Table 1.1) are indicative of a hydrophobic behaviour and high affinity for organic carbon, such as sediments and lipid-like substances. Additionally, both HHCB and AHTN can be considered semivolatile compounds, according to Weschler et al. (2008), who defined semivolatiles as compounds with a vapor pressure between 10^{-9} and 10 Pascals (Pa). Both musks also possess boiling points higher than water, a characteristic of semivolatile compounds, and therefore they may volatilize when exposed to temperatures above room temperature (EPA, 2015). Semivolatile organic compounds include some phenols and polycyclic aromatic hydrocarbons (PAHs), like

fluoranthene and pyrene, which possess vapor pressures ($1.23 \cdot 10^{-3}$ and $0.60 \cdot 10^{-3}$ Pa at 25°C) comparable to those of HHCB and AHTN.

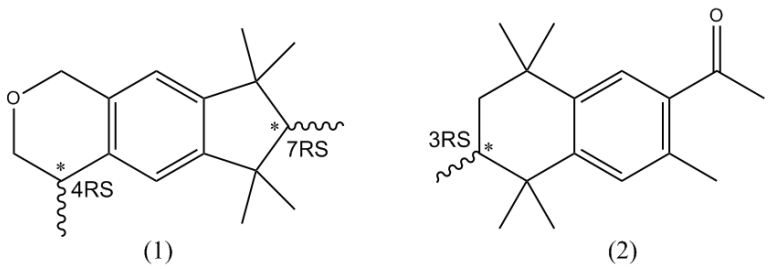

Figure 1.1. Structures of polycyclic musks (1) HHCB and (2) AHTN. The stars represent the chiral centers, at positions 4 and 7 for HHCB and position 3 for AHTN

Table 1.1. Physicochemical properties of synthetic fragrances HHCB and AHTN

Properties	HHCB	AHTN	Units
Molar mass[1]	258.4	258.4	$g \cdot mol^{-1}$
Skeleton type	Indane	Tetralin	N/A
Chiral center positions[2]	4, 7	3	N/A
Log K_{ow}[3]	5.9	5.7	N/A
Log K_{oa}[4]	8.17	7.95	N/A
Vapor pressure[3]	0.0727	0.0608	Pa
Water solubility[3]	1.75	1.25	$g \cdot m^{-3}$
Melting point[1]	-10	54	°C
Boiling point[1]	325	180	°C
Half-Lives			
Atmospheric[5]	3.4	7.3	h
Water[6]	33-43	N/A	h
Sediment[7]	1,896	N/A	h
Bluegill Sunfish	2-3	0.8-2.1	d

[1] HERA, 2004
[2] Frater, 1999
[3] Balk et al., 1999a
[4] Estimated with KAOWIN© software (Boethling, 2011)
[5] Aschmann et al. (2001)
[6] Langworthy et al., 2000
[7] Envirogen, 1998

The product of synthesis for HHCB is a racemic mix of two diastereoisomeric pairs of enantiomers, which are (4S,7R) *vs.* (4R,7S) and (4S,7S) *vs.* (4R,7R). It is known that the musky fragrance is strongly expressed by the two diastereoisomers (4S,7R) and (4S,7S) (Frater et al., 1999). Low selectivity between

these two pairs of diastereoisomers occurred when biotransformation was allowed in fish and sludge (Gatermann et al., 2002). In addition, all the enantiomers seemed to be equally bioaccumulated by fish (Franke et al., 1999; Bester, 2005).

1.5. Environmental fate and degradation of HHCB and AHTN

Structural features and physicochemical properties are usually good predictors of the environmental fate of contaminants when data are not available, as well as measured degradation time by abiotic factors: reaction in water, air and sediment (Table 1.1). However, accumulation and biotic degradation, or biotransformation, will vary with the species. An experiment was conducted on the benthic invertebrate *Chironomus riparius*, exposed to high concentrations of musks in a flow-through system (9.8 $\mu g \cdot L^{-1}$ HHCB and 5.8 $\mu g \cdot L^{-1}$ AHTN). The comparison between bioconcentration factors (BCFs) obtained with the addition of piperonyl butoxide (PBO), a biotransformation inhibitor, and the ones obtained without addition of PBO, showed that biotransformation of HHCB and AHTN was occurring in this species of invertebrate: the BCF values were higher with the addition of PBO. With PBO, BCF for HHCB and AHTN were respectively 525 and 7,943, whereas without PBO, i.e. with biotransformation, BCF values for HHCB and AHTN ranged respectively from 85 to 138 and from 50 to 112. The worm *Lumbriculus variegatus*, exposed to water concentrations of 4 $\mu g \cdot L^{-1}$, showed BCF values of 2,692 for HHCB and ~3000 for AHTN after 3 days of exposure. These were indicative of the absence of biotransformation occurring in this species of worm as they were the same magnitude as predicted BCFs, the latter based on lipid content and octanol-water partition coefficients (log K_{ow}) (HERA, 2004).

The main product of abiotic degradation and biotransformation of HHCB is HHCB-lactone, or Galaxolidone (Figure 1.2). The benzylic methylene group of HHCB is oxidized to a more polar form, resulting in a lactone group. To our knowledge, no other degradation product for HHCB has been identified. HHCB-lactone was quantified in surface water and fish, at levels between 20 and 30 $ng \cdot L^{-1}$ (Bester, 2005; Franke et al., 1999). Janzen et al. (2011) found that the degradation time for HHCB-lactone (120 minutes) was longer than for the parent musk HHCB (20 minutes) when reacting with ozone directly. To our

knowledge, the toxicity of HHCB-lactone has not been investigated yet. Degradation products of AHTN have been synthetized and characterized (Valdernes et al., 2005), and also quantified in breast milk and fish samples. The concentrations varied between 7 to 24 $pg \cdot g^{-1}$, and to our knowledge, very few studies have examined AHTN transformation products in environmental sample (Santiago-Morales et al., 2013). AHTN is degraded by ozonation after a reaction time of 120 minutes (Janzen et al., 2011).

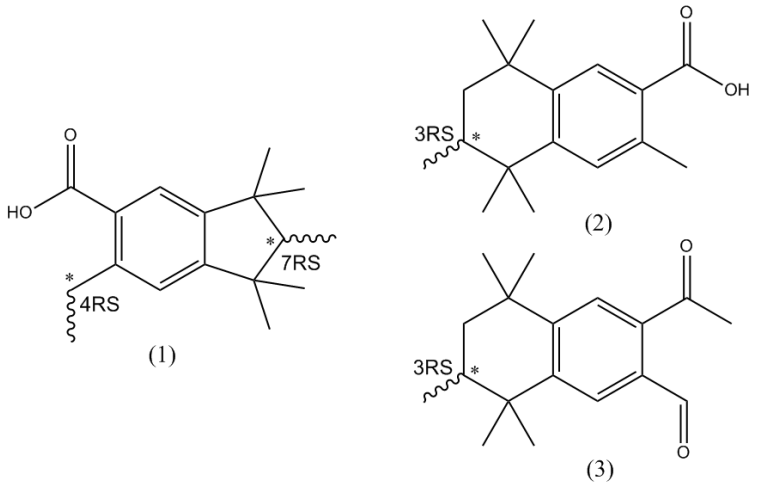

Figure 1.2. Structures of degradation products of polycyclic musks: (1) HHCB-lactone and (2; 3) two degradation products of AHTN (no name assigned). The stars represent the chiral centers, at positions 4 and 7 for HHCB sub-product and position 3 for AHTN sub-products.

1.6. HHCB and AHTN toxicity mechanisms

1.6.1. Acute and sublethal toxicity

Adverse effects have been previously observed in invertebrate species exposed to synthetic musks. In particular, toxicity to earthworm *Eisenia fetida* was investigated using traditional and molecular endpoints: according to Chen et al. (2011), median lethal concentrations (LC_{50}) after 14 days of exposure were 392.4 and 436.3 $\mu g \cdot g^{-1}$ dried soil, for HHCB and AHTN respectively. These high concentrations may not occur in the environment, however sublethal effects such as the up-regulation of superoxide dismutase (SOD) and catalase (CAT), scavengers of stress-induced reactive oxygen species, were shown to happen at lower concentrations by the same study. A 28-day exposure experiment to levels of 30, 50 $\mu g \cdot g^{-1}$ of HHCB and AHTN in soil showed a significant increase of SOD and CAT enzymes in *Eisenia fetida*. Relatively

similar levels of HHCB and AHTN have been found in dry sludge, such as 82 and 34 $\mu g \cdot g^{-1}$, respectively, which is being used on agricultural soil (Shek et al., 2008). HHCB and AHTN also showed toxicity in the nematode *Caenorhabditis elegans*. The lowest observed effect concentrations (LOECs) on growth, maturation and reproduction varied between 6.4 and 25.5 $mg \cdot L^{-1}$, HHCB being generally slightly more toxic than AHTN (Mori et al., 2006). In the copepod *Arcatia tonsa*, the early copepodite stage development was inhibited at half maximal effective concentrations (EC50) of 0.059 mg HHCB $\cdot L^{-1}$ and 0.026 mg AHTN $\cdot L^{-1}$ during a 5 days exposure (Wollenberger et al., 2003). These levels are one order of magnitude higher than the highest STP effluent concentrations (up to 0.0021 $mg \cdot L^{-1}$ in the UK, Sumner et al., 2010).

Agricultural soil contaminated with polycyclic musks may also affect plants. Subsequently to HHCB exposure from 50 to 250 $mg \cdot L^{-1}$, the shoot and root elongations of wheat (*Triticum aestivum L.*) were significantly inhibited (An et al., 2009). A 21-day exposure experiment in wheat seedlings at lower levels (0.2 to 3.0 $mg \cdot L^{-1}$ HHCB) caused a decrease in chlorophyll during growth and soluble protein concentrations, which may lead to metabolism disorders in wheat (An et al., 2009).

1.6.2. Endocrine disruption of synthetic musks

HHCB and AHTN were both reported to display endocrine disrupting activities in male and female fish to varying degrees, however, since HHCB is found in the environment at much higher concentrations than AHTN (Chapter 3), the risk posed by HHCB is greater than AHTN. Hence, this section focused more toward HHCB endocrine disruptive properties than AHTN. Simmons et al. (2010) exposed modified yeast containing the human estrogen receptor α (hERα) to the commercial formulation used in cosmetic and pharmaceuticals, a HHCB and phthalates mixture, and measured the response. This mixture alone was able to trigger an estrogenic response up to 15% of the maximum response induced by 17β-estradiol (E2), the natural substrate of the receptor, at concentrations two orders of magnitude higher than E2. The exposure of the hERα to both the mixture and E2 revealed HHCB's antagonistic behavior, by competition with E2 at the receptor binding sites. Simmons et al. (2010) confirmed this dose-dependent competition mechanism by assessing vitellogenin level changes in female rainbow trout, an egg yolk protein precursor which is an

indicator of the activation of ERα. Vitellogenin concentrations were significantly lower in fish injected with HHCB and E2 compared to the positive control fish in which E2 alone was injected. This result was indicative of competitive binding antagonism.

Schreurs et al. (2002) found both HHCB and AHTN to act as selective estrogen receptor modulators (SERMs) when tested with *in vitro* reporter gene assays, which implies either estrogenic or antiestrogenic behavior depending on the cell line and the estrogen receptor subtype used (ERα or ERβ). Both HHCB and AHTN displayed estrogenic behavior in HEK293 cells by activating transcription at ERα at very high concentrations of 10 μM (Schreurs et al., 2002). Transcription at ERβ was not activated. Antiestrogenic behaviour was caused by substrate competition at binding sites of both ERα and ERβ in two types of cell lines (U2-OS and HEK293). Strongest antiestrogenic effects were observed at ERα in HEK293 cells, with half-maximal inhibitory concentrations (IC50) of $2.4 \cdot 10^{-5}$ and $2.1 \cdot 10^{-5}$ M (ERα) for AHTN and HHCB respectively (Schreurs et al., 2002). Schreurs et al. (2005) found HHCB and AHTN to antagonise all the receptors tested, i.e. the estrogen, progesterone and androgen receptors, with more potency toward the progesterone receptor. Although most of the half-maximal inhibitory concentrations (IC50) were relatively high, AHTN-caused anti-progestagenic effects were observed at concentrations as low as 0.01μM, with an IC50 of 24 nM (Schreurs et al., 2005). In a reporter gene assay testing for the estrogenic and antiestrogenic potency of HHCB and AHTN, both musks showed antiestrogenic behavior on the androgen receptor (AR), estrogen receptor β (ERβ) and progesterone receptor (PR), with more potency toward PR (Van der Burg et al., 2008). The effects of both musks on the PR were stronger than most of the other antagonists tested, i.e., viclozolin, methoxychlor, HPTE, and two forms of DDT, but were lower than the PR reference antagonist used (RU486). While the consequences of antagonistic activity caused by foreign chemicals binding to PR are currently unknown, the potency of musks toward PR is only ten times lower than the major PR antagonistic natural ligand, Org2058 (Van der Burg et al., 2008).

Synthetic musks HHCB and AHTN are also known to affect the male endocrine system. Endocrine disruption was reported in male Medaka fish (*Oryzias latipes*) exposed to concentrations of 500 $\mu g \cdot L^{-1}$ HHCB and AHTN, as the production of vitellogenin in the liver and mRNA related to the ERα both

increased. The induction of vitellogenin in male Medaka fish is a strong indication of endocrine disruption caused by musks, although the toxicological consequences of this activity have not been related clearly to reproductive impairment (Yamauchi et al., 2008). Fernandes et al. (2013) investigated enzyme activity changes in the male European sea bass *Dicentrarchus labrax* exposed to HHCB, and found that the enzymes Cyp17 and Cyp11β were both inhibited to a significant extent. During sexual maturation, Cyp17 catalyzes the production of androstenedione, which leads to testosterone, as Cyp11β transforms both of these into their hydroxylated metabolites. In European sea bass, the Cyp11β enzyme synthesis is normally elevated at the early stages of sexual maturation, and changes may alter androgen related biological processes like spermatogenesis, reproductive behavior and the development of secondary sexual characteristics. The inhibition of the activity of these two enzymes in the presence of HHCB was also observed in male carp by Schnell et al. (2009). Another noteworthy consequence of exposure is observed in the species of earthworm discussed above (*Eisenia fetida*). A significant decrease in cocoon production occured at concentrations of 50 μg AHTN·g^{-1} soil and 100 μg HHCB·g^{-1}. Annetocin, a peptide structurally and functionally related to the vertebrate hormone oxytocin, is related to egg-laying behaviour in earthworm and was about 4 times lower in concentration when exposed to 100 μg·g^{-1} of either HHCB or AHTN (Chen et al., 2011).

1.6.3. Other toxicity mechanisms

Toxicity of polycyclic musks in marine mussels (*Mytilus californianus*) was observed at the multixenobiotic transporters, which are cell membrane proteins responsible for elimination of foreign compounds. Transporters were inhibited in a dose-dependent manner when exposed to musks, at doses of 1 and 10 μM. The inhibition of these transporters allows the accumulation of foreign compounds in the cell, which may increase their toxic action potential (Luckenbach et al., 2004).

The toxicity of HHCB in the presence of cadmium (Cd) has been investigated in wheat seedlings. Chen et al. (2014) found that high concentrations of HHCB increased the accumulation of Cd and their combination could potentially increase phytotoxicity in wheat seedlings, by affecting chlorophyll, lipid peroxidation and antioxidant enzymes. The induction of antioxidant stressors such as superoxide dismutase

(SOD), peroxidase (POD) and malondialdehyde (MDA) by the combination of these contaminants in fish has also been examined (Zhang et al., 2012; Chen et al., 2012), but more research is needed to determine if any synergistic activity is occurring.

1.7. Bioaccumulation

Bioaccumulation is defined as the net result of the competing rates of chemical uptake, whether at the respiratory surface (e.g. gills in fish) or from the diet, and the chemical elimination by several pathways (Arnot et al., 2006). However, the dietary uptake is not part of the pathways accounted in the calculation of the bioconcentration factor (BCF) (Arnot et al., 2006). The physicochemical properties of HHCB and AHTN, such as the log K_{ow}, their slow elimination rates and their tendency to be present in several environmental compartments make them good candidates for bioconcentration and bioaccumulation in fish. The log K_{ow} endpoint defined by Environment Canada and the United Nations Environment Program (1999) for bioaccumulative substances is 5 or higher, and HHCB and AHTN would fall in that category with log K_{ow} of 5.9 and 5.7 respectively. Boethling (2011) characterized the bioaccumulation potential of polycyclic musks with the BCFBAF estimation software, and classified it as high to very high. Previous publications reporting BCFs and BAFs in urban areas (Klaschka et al., 2013; Gatermann et al., 2002) showed great variation between species, with BAFs from 20 to 1,584 for HHCB and from 40 to 670 for AHTN (Zhang et al., 2013). The risk associated with exposure varies depending on the extent of bioaccumulation, which is why the persistence and presence of musks need to be monitored in urbanized areas. This project aimed to provide information on the potential exposure and toxicity risks of synthetic musks to surface water in contaminated urban areas.

Chapter 2

2. Method development for purification and quantification of the synthetic musks HHCB and AHTN in whole fish tissue

2.1. Abstract

A method for clean-up of fish samples was optimized with deuterated fluoranthene as a recovery standard, in order to remove interferences for the quantification of polycyclic musks HHCB and AHTN. This procedure was performed firstly by pressurized fluid extraction (ASE-200) followed by automated gel permeation chromatography (GPC) for lipid removal. Post GPC, purification with alumina neutral was used to remove additional matrix interferences. Mean recoveries in fresh salmon spiked with musks prior to extraction were 74.2% for HHCB, with a relative standard deviation (RSD) of 12.2%, and 134.5% with a RSD of 5.2% for AHTN. The recovery for d10-fluoranthene was 68.2 %, with a RSD of 2.0%. All-in-one cell pressurized fluid extractions executed with alumina neutral sorbent were also attempted and failed to remove most lipids. Another method combining ASE, gel permeation chromatography and Florisil chromatography succeeded in eliminating fish matrix interferences but gave low and variable recoveries for HHCB, AHTN and d10-fluoranthene. Alkaline digestion resulted in a thick viscous sample which prevented further analytical procedures.

2.2. Introduction

Synthetic musks 1,3,4,6,7,8-hexahydro-4,6,6,7,8,8-hexamethylcyclopenta(g)-2-benzopyrane (HHCB) and 7-acetyl-1,1,3,4,4,6-hexamethyltetrahydronaphtalene (AHTN) are the most detected fragrances in sewage treatment plant effluents, with a production of over 4,500 tons per year according to the high production-volume chemicals list compiled by the US Environmental Protection Agency (EPA). Given their potential for endocrine disruption (Simmons et al., 2010; Schreurs et al., 2005; Van der Burg et al., 2008) and their hydrophobic properties (log K_{ow} of 5.9 and 5.7 for HHCB and AHTN respectively), concern is rising over the potential for bioaccumulation in exposed biota. To assess this potential, methods

to quantify HHCB and AHTN in several environmental media such as water and sediments (Sumner et al., 2010), soil (Chen et al., 2014), dust (Fromme et al., 2004), air (Peck et al., 2006) and fish (O'Toole et al., 2006) have been developed, however, a discrepancy exists toward the usage of d3-AHTN as a recovery standard. D3-AHTN, which is synthetized by the exchange of protons to deuterons, has been reported to undergo proton exchange during sample processing and storage, therefore reverting back to its undeuterated form (Buerge et al., 2003; Bester, 2005; Bester, 2009). Inadequate separation and mass spectral interferences between deuterated internal musk standard and target analytes were also reported (Peck et al., 2007). Despite this potential problem, other studies have successfully quantified musks in environmental media, with recoveries ranging from 85 to 108% in water (Clara et al., 2011), from 92 to 108% in sludge (Clara et al., 2011), from 59 to 100% in suspended particulate matter samples (Sumner et al., 2010) and from 89.7 to 104.9% in surface water (Hu et al., 2011). Other publications used deuterated polycyclic aromatic hydrocarbons (PAHs) as recovery and internal standards with success. D10-fluoranthene showed an average recovery of 76 ± 12% in airborne particulate-phase (Peck et al., 2004), 78 ± 6% in various tested standard reference materials, which were mostly biota (Peck et al., 2007). D10-phenanthrene recoveries ranged from 65 to 90% in high trophic level aquatic organisms (Kannan et al., 2005). The discrepancy involving standards was addressed in this chapter by adapting a method to quantify HHCB and AHTN in whole fish homogenate with deuterated PAHs d10-fluoranthene as a recovery standard and d10-pyrene as an internal standard. Three trials are included in this chapter and discussed.

2.3. Experimental

2.3.1. Standards and reagents

Analytical grade solutions of HHCB and AHTN in 2,2,4–trimethylpentane were purchased from ULTRA Scientific at 98% purity. Recovery and internal standards solutions of d10-fluoranthene (98%) and d10-pyrene (98%) in 2,2,4-trimethylpentane were purchased from Cambridge Isotope Laboratories Inc. Optima grade solvents (acetone, n-hexanes, dichloromethane, ethyl acetate, dimethyl sulfoxide, petroleum ether and 2,2,4–trimethylpentane) were all purchased from Fisher Scientific. Diatomaceous earth

(Hydromatrix) was purchased from Agilent technologies, rinsed thoroughly with petroleum ether and dried before use. Anhydrous granular sodium sulfate (certified ACS) and neutral aluminum oxide with 60-325 mesh size (Brockman Activity I) were both purchased from Fisher Scientific. Florisil® (60/100 mesh size) was purchased from Supelco. All glassware used was rinsed with polar and non polar solvents and baked prior to usage in order to avoid cross contamination.

2.3.2. Fish spiking and homogenization

In the absence of available standard reference material in a biotic matrix, fish species were spiked with musks in order to execute method trials. Live adult goldfish *Carrasius auratus auratus* (n=9) (sex not determined) were injected intraperitoneally with a measured approximate of 1 $\mu L \cdot g^{-1}$ (body weight) solution of both HHCB and AHTN in dimethyl sulfoxide (DMSO) at different concentrations. These goldfish were used as standard reference materials in order to test the method efficiency by measuring HHCB and AHTN recoveries. Doses ranged between 10 and 95 $ng \cdot g^{-1}$ fish, and chemicals were allowed to spread in the organism for 15 minutes prior to their euthanasia with tricaine methanesulfonate (MS-222). Three additional goldfish, which were not injected with musks, were euthanized and processed as control fish. This work was conducted under an animal care permit in the aquatic animal facilities at the University of Ottawa. Fresh goldfish weighing on average 19 ± 2 g were then homogenized and frozen until used. Thawed homogenate was then subsampled in 1 to 2 grams of biomaterial and were used to test analytical procedures for the quantification of HHCB and AHTN in fish biological matrix.

The successful analytical procedure was then applied to fathead minnow (FHM) carcasses (1.76 ± 0.09 g), which were provided by colleagues at the University of Alberta, in order to assess the extent of musk bioaccumulation in exposed/ stressed biota. Collection and handling were described elsewhere (Jasinska et al., 2015). Briefly, native FHMs were harvested from a pond in the North Saskatchewan River watershed and kept two weeks in the aquatic facility at the University of Alberta prior to deployment. Fathead minnows were deployed upstream and downstream of the Gold Bar wastewater treatment plant in Frabill© bait buckets for a period of four weeks, from September 13 to October 13, 2011. During the entire

process, fish were fed with 1 mm trout pellets. Finally, fish were sacrificed with MS-222 and kept at -80°C until homogenization, executed with a knife and board to insure minimal sample loss. Due to their small size, the whole body was processed for quantification of HHCB and AHTN.

2.3.3. Protocol #1: all-in-one cell approach

A more classic method for characterization of contaminants in environmental samples can involve two or three steps, for extraction, lipid removal and clean-up. Here, the extraction and lipid removal steps, for quantification of musks in fish, were combined in one step, as performed by Draisci et al. (1998). This combination, was used in order to reduce sample preparation time, as the intent is the elimination of most non-polar impurities while samples are being extracted with automated pressurized fluid extraction (PFE). This would allow the extracts to be directly injected to a gas chromatograph (Agilent Model 6890 series) coupled to a triple quadrupole mass selective detector (Agilent Model S973), or GC-MSD. This combined procedure was tested on goldfish samples using the Accelerated Solvent Extractor 200 (ASE 200). First, neutral aluminum oxide (alumina) was activated at 500°C for 4 hours and 15, 9, 6 or 3% deactivated (w/w) with pure HPLC grade water. Then, 5 or 7.5 g of alumina was added as a bottom layer in individual 33 ml stainless steel extraction vessels (ASE cells). One to two gram subsamples of whole fish homogenate were mixed with Hydromatrix and added over either 5 or 7.5 g alumina in the ASE cells. A cellulose filter prevented the mixing of these two layers. Every extraction vessel was spiked with 20 ng of recovery standard d10-fluoranthene prior to extraction performed with settings presented in Table 2.1. Goldfish extracts resulting from this procedure were left to dry overnight in pre-weighed aluminum cups in order to measure the extracted lipid content.

Table 2.1. Extraction parameters used in the all-in-one cell approach for the analysis of HHCB and AHTN in spiked goldfish with ASE-200.

Extraction solvent	1:5 EA: Hex (v/v)
Temperature	80°C
Pressure	1450 psi
Heat time	5 min
Static time	5 min
Flush volume	100%
Purge time	90 s
Static cycles	2

2.3.4. Protocol #2: GPC coupled to Florisil chromatography

Pressurized fluid extraction was performed on goldfish with ASE-200 and was adapted from Peck et al. (2006). ASE cells (33 ml capacity) were packed with 1 to 2 g goldfish subsamples mixed with either sodium sulfate (Na_2SO_4) or Hydromatrix. Each sample was spiked with 20 ng of recovery standard d10-fluoranthene prior to extraction, with conditions reported in Table 2.2. Extracts were then subjected to gel permeation chromatography (GPC) to remove lipids and macromolecules co-extracted with the compounds of interest. This step was adapted from O'Toole et al. (2006). Briefly, extracts were reduced to 2 ml at 35°C with nitrogen (TurboVap® II, Zymark Hopkinson, MA, USA) and loaded on 60 g of SX-3 Biobeads contained in a 2.5 cm i.d. × 50 cm glass column. Elution was carried with a mobile phase of 1:1 ethyl acetate: hexanes at 2 $ml \cdot min^{-1}$. The first 50 ml fraction was collected as it contained d10-fluoranthene. The following 60 ml fraction was discarded (lipids) and the last 50 ml fraction (HHCB and AHTN) was collected and combined with the first fraction prior to evaporation to 1 ml. Further clean-up was accomplished by Florisil gel column chromatography, and was based on a method published by O'Toole et al. (2006). Columns were packed from bottom to top with glass wool, 6 g of activated Florisil pre-heated 6 hours at 300°C, and 1g of anhydrous sodium sulfate (Na_2SO_4). Samples were eluted with 80 ml of ethyl acetate which was collected and reduced to 0.5 ml for quantitation by GC-MSD. The gas chromatograph was equipped with a 26.7 m × 0.25 mm DB-5MS (film thickness: 0.25 µm) capillary column (model number J&W 122-5532). The injector temperature was set to 250ºC and injections of 2 µL were done with splitless mode. Helium was used as the carrier gas at a flow of 2 $ml \cdot min^{-1}$. The temperature program was as follows:

the column heated from 90ºC to 180 ºC at 10ºC·min^{-1}, ramping up to 210ºC at 2ºC·min^{-1}, then up to 290ºC at 30ºC·min^{-1}. The transfer line temperature was set to 300ºC and the quadrupole and detector source were set to 150 and 230 ºC respectively. The following ions were isolated by selective ion monitoring as quantitative (first ion) and qualitative: 243 and 213 for HHCB, 243 and 258 for AHTN, 212, 208 and 210 for d10-fluoranthene and 212, 208 and 210 for d10-pyrene.

Table 2.2. Extraction parameters used in protocol #2 for the analysis of HHCB and AHTN in spiked goldfish with ASE-200.

Extraction solvent	Dichloromethane
Temperature	100°C
Pressure	2,000 psi
Heat time	5 min
Static time	5 min
Flush volume	100%
Purge time	90 s
Static cycles	2

2.3.5. Protocol #3: alkaline digestion

Additional goldfish subsamples were extracted as described previously in protocol #2. Alkaline digestion was then employed (Martinez et al., 2004) to remove co-extracted interferences and lipids. A 20 ml volume of KOH 6M was added directly to the extracts which were then shaken vigorously for 18 hours. Following the digestion, liquid-liquid extraction was performed using 3 fractions of 20 ml of hexane, which were then combined. Due to the presence of visible water droplets at that stage, combined fractions were filtered through approximately 6 g of sodium sulfate for water removal, then evaporated down to a volume of 0.5 ml. Due to practical reasons, no further purification or GC-MS analysis was performed.

2.3.6. Protocol #4: automated GPC coupled to alumina chromatography

This procedure was performed on exposed fathead minnows (FHMs) from the North Saskatchewan River, and the results were discussed in Chapter 3. Pressurized fluid extraction was performed with the ASE-200 within 24 hours of sample homogenization. Whole fathead minnows were used, as opposed to subsamples, as FHMs weight ranged mostly from 1 to 2 g. Fish homogenate was mixed with Hydromatrix

and each 11 ml cell was spiked with 20 ng of deuterated polycyclic aromatic hydrocarbon (PAH) d10-fluoranthene, prior to extraction to assess the method recovery (Table 2.3). FHM extracts were evaporated down to 1 ml, and the removal of residual water and particulates prior to chromatography was done by filtration through a Chromafix cartridge containing 1 g of sodium sulfate (Na_2SO_4) connected to a 0.2 µm polytetrafluoroethylene (PTFE) filter. Cartridges and filters were rinsed twice with approximately 1 ml of dichloromethane (DCM). Prior to injection, sample volume was topped to 4 ml. All samples were run in two injections of 2 ml, on two connected Envirogel™ columns (19 × 150 mm → 19 × 300 mm) (Waters Corporations, MA, USA). Dichloromethane, which was sonicated for 20 min before usage, was used as the mobile phase at 8 $ml \cdot min^{-1}$ and 48 bar of pressure. Injections were done with a 2 ml loop auto sampler device integrated in the Agilent 1200 Series preparative HPLC system which also regulated flow rate and pressure. Fraction collection was confirmed with UV detection screening at 254 and 360 nm. Most of the lipid fraction was discarded. Post lipid removal, clean-up of FHM extracts with alumina columns was performed, adapted from Hu et al. (2011). Custom-made glass columns (i.d. 11.9 mm, 77 mm lenght) were dry-packed and mounted from bottom to top with glass wool, 4 g of alumina neutral and 1 g of anhydrous sodium sulfate (Na_2SO_4). Alumina was previously activated at 500ºC for 4 hours and 3% (w/w) deactivated with HPLC grade water. Dry packed columns were then conditioned with 5 ml of n-hexanes prior to sample loading. FHM samples, reduced to 0.5 ml in 2,2,4-trimethylpentane (TMP) with TurboVap® II, were added onto the column, followed by a 0.5 ml n-hexanes rinse. Elution was performed with 4.5 ml of n-hexanes followed by 20 ml of a mixture of n-hexanes/ dichloromethane (2:1). Collected fractions were reduced to 0.5 ml TPM, transferred to 1.5 ml amber vials and prepared for GC-MSD analysis. Quantification with GC-MSD was performed as reported in section 2.3.4 (Protocol #2).

Table 2.3. Extraction parameters used in the analysis of HHCB and AHTN in exposed fathead minnows with ASE-200. The mixture of optima grade ethyl acetate (EA) and n-hexanes (Hex) was made prior to extraction.

Extraction solvent	1:5 EA: Hex (v/v)
Temperature	80°C
Pressure	1,500 psi
Heat time	5 min
Static time	10 min
Flush volume	100%
Purge time	90 s
Static cycles	2

2.3.7. Method validation

Prior to application of protocol #4 on exposed fathead minnows from the North Saskatchewan River, the method was validated with several sample extractions. To save time and resources, a salmon filet was purchased from a local grocery store and used for method validation. Skin was removed and the filet was homogenized with a commercial blender. Every 1 to 2 g subsamples were spiked with 50 ng each of HHCB, AHTN and d10-fluoranthene. In order to produce comparable results, chemicals were mixed with fish tissue directly and allowed to bind to the matrix for 15 minutes, prior to addition of the dispersing agent (Hydromatrix). Two method blanks were processed with each extraction performed with ASE-200, and one was spiked with the recovery standard. Care was taken in the laboratory to minimize contamination by musks from personal care and cleaning products. Concentrations were blank subtracted.

2.4. Results and discussion

2.4.1. All-in-one cell approach

The all-in-one cell approach (Protocol #1) was not further considered for the analysis of HHCB and AHTN because the test goldfish extracts contained too many interferences and were not suitable for GC-MS analysis. In the samples extracted with 15% deactivated alumina, oily/ yellow coloured residues were found after the evaporation of extracts. As a result, further purification would have been needed for quantification by GC-MS, to avoid clogging the system and reducing column life. The addition of steps like lipid removal defeated the initial purpose of this method, which was employed to save time and

resources. Harsher sorbent conditions such as enhanced Brockman activity alumina (9, 6, 3%, and no deactivation) and larger amounts (7.5 g instead of 5 g) consistently resulted extracts containing oily residues. This inefficiency may have been due to sample humidity as they were derived from fresh fish homogenate. Since water is acting as a deactivating agent for alumina, humidity contained within the sample may have neutralized binding sites and affected the lipid retaining capacity. Our samples may have had a higher intrinsic humidity than samples tested in Draisci et al. (1998). This could have deactivated the alumina bed to a greater extent. This could have been the reason why the all-in-one cell approach did not work for us, although it seemed to have retained lipids successfully in samples from Draisci et al. (1998).

2.4.2. GPC coupled to Florisil chromatography

Protocol #2 showed poor and variable recoveries (Table 2.4). The high relative standard deviations reflect a high variability and low reproducibility of the method. Overall, recoveries ranged from 5 to 66% for HHCB and 14 to 53% for AHTN. In addition, the mean recoveries of d10-fluoranthene were not consistent with each other and were not consistent with HHCB and AHTN recoveries. These results could be attributed to the usage of Florisil chromatography. As Florisil was part of a successful method in the determination of musks in fish samples without the use of deuterated PAHs (O'Toole et al., 2006), another publication (Rimkus, 1999) reported variably high losses of polycyclic musks due to adsorption to Florisil. In our case, d10-fluoranthene could have adsorbed to activated Florisil, causing lower and variable recoveries. PAHs such as benzo(a)pyrene (MW of 252.31 $g \cdot mol^{-1}$) and benzo(ghi)perylene (MW of 276.33 $g \cdot mol^{-1}$), when eluted with n-hexanes and mixtures of n-hexanes: DCM at varying ratios, were found to have poor recoveries due to adsorption to Florisil (Bucszynska et al., 2015). Bucszynska et al. (2015) reported excellent recoveries for fluoranthene (MW of 202.26 $g \cdot mol^{-1}$) when working with Florisil. However, d10-fluoranthene as a larger molecular weight (212.21 $g \cdot mol^{-1}$) than its undeuterated form, and this feature, increasing retention to the Florisil gel, may have resulted in low and variable recoveries.

Table 2.4. Mean recoveries of HHCB, AHTN and d10-fluoranthene in injected goldfish (*Carrassius auratus auratus*) analyzed with protocol #2. Standard error (SE) is given in parenthesis. The number of fish subsamples (n) and the relative standard deviation (%RSD) are also given.

Spiking level	HHCB			AHTN			d10-Fluoranthene		
ng/g	% Rec	n	%RSD	% Rec	n	%RSD	% Rec	n	%RSD
Blank	NA	NA	NA	NA	NA	NA	54.3 (12.2)	2	31.8
0	NA	NA	NA	NA	NA	NA	20.0	1	NA
10	46.0 (7.9)	2	24.1	27.7 (1.4)	2	26.5	20.9 (1.7)	3	59.6
15	21.7 (1.6)	6	17.6	12.5 (1.3)	6	24.8	41.4 (17.0)	4	82.0
95	15.2 (3.9)	6	63.2	12.2 (3.3)	6	65.9	16.3 (5.7)	6	85.4

2.4.3. Alkaline digestion

For practical reasons, protocol #3 was not used in the determination of HHCB and AHTN in fish samples. Following digestion with KOH 6M and liquid-liquid extraction, the evaporation of the combined fractions resulted consistently in a thick, coloured, jelly texture in a volume of 0.5 ml to 1 ml. Martinez et al. (2004) reported similar problems, i.e.: in the event a coloured viscous sample was obtained, the samples were subjected to further clean up by solid phase extraction (SPE) with alumina. We did not proceed with SPE alumina purification because of the high thickness of the samples, which was also a problem when reconstituted in 1.5 ml n-hexanes. Also, as the SPE method described in Martinez et al. (2004) was adapted to PAHs rather than musks, additional work would have been needed in order to adapt a SPE method for the purification of thick samples.

2.4.4. Protocol #4 and method validation

Following validation, this method was employed for the determination of HHCB and AHTN in fathead minnow samples. HHCB and d10-fluoranthene recoveries were consistent and had low standard errors and relative standard deviations (RSD), which meant a good reproducibility in both cases (Table 2.5). Despite a mean recovery of 134.5% obtained for AHTN, the standard error and the RSD associated with this value were in the same range as the ones obtained for HHCB and d10-fluoranthene. The method detection limits were 6.2 and 2.0 $ng \cdot g^{-1}$ (ww) fish for HHCB and AHTN, respectively.

Table 2.5. Mean recoveries of HHCB, AHTN and d10-fluoranthene in spiked salmon filet analyzed with protocol #4. Standard error (SE) is given in parenthesis. The number of fish subsamples (n) and the relative standard deviation (%RSD) are also given.

	HHCB	AHTN	d10-Fluoranthene
Recovery (%)	74.2 (3.4)	134.5 (5.2)	68.2 (2.0)
n	7	7	7
% RSD	12.2	10.2	7.7

2.5. Conclusion

A reliable method for clean-up of fish media and quantification of HHCB and AHTN with a PAH recovery standard was determined. This method involved the use of pressurized fluid extraction, automated liquid chromatography, SPE with alumina neutral and gas chromatography coupled to mass selective detection, which resulted in good reproducibility and low variability in the recoveries. This work underlined the following problems when working with musks and deuterated PAH recovery standards. The all-in-one cell extraction approach, using alumina neutral, failed in removing lipids and interferences when extracting fresh fish samples. Florisil chromatography was not a suitable option when using d10-fluoranthene as a recovery standard, since the Florisil may retain the compounds in an irreversible way and induce variation in the recoveries.

Chapter 3

3. Presence and bioconcentration of polycyclic musks HHCB and AHTN in fathead minnows (*Pimephales promelas*) from the North Saskatchewan River, Edmonton

3.1. Abstract

HHCB and AHTN are synthetic fragrances used in a wide variety of common products and are among the most abundant personal care products released to the environment (Del Río et al., 2013). Their presence in urban environments and hydrophobicity are raising concern about their bioaccumulative potential and capacity to cause endocrine disruption in aquatic species. HHCB and AHTN levels were examined in fathead minnows (FHMs) exposed for a month in a contaminated area in the North Saskatchewan River in Edmonton, near the Gold Bar wastewater treatment plant (GBWWTP). Both musks, HHCB and AHTN, were present in water and fathead minnows at the furthest site, 9.9 km downstream of effluent. Highest concentrations were found in FHMs exposed at the outfall site and were comparable to effect doses reported in female rainbow trout. Both musks, HHCB and AHTN, were present in water and fathead minnows at the furthest site, 9.9 km downstream of the outfall. Bioconcentration factors (BCFs) were the highest at the outfall site, and calculated BCFs in FHMs from the downstream sites, at 2.5 and 9.9 km, were the lowest. This suggested that FHMs exposed to lower fragrance levels were able to biotransform and excrete HHCB more efficiently. Bioconcentration occurred in FHMs exposed at both reference sites, upstream GBWWTP. Musk ratios in water and in fish across the sites were compared and seemed to underline differences in biotransformation and elimination of musks in fish.

3.2. Introduction

With industrial development and populations, concern is growing toward the impact of the increasing amount and variety of pharmaceuticals and personal care products released in the environment. Among endocrine disrupting chemicals from personal care products, Galaxolide, or 1,3,4,6,7,8-hexahydro-4,6,6,7,8,8-hexamethylcyclopenta(g)-2-benzopyrane (HHCB) and Tonalide, or 7-acetyl-1,1,3,4,4,6-hexamethyl-tetrahydronaphtalene (AHTN) are synthetic fragrances added to common personal care and

household cleaning products, at levels of 1,427 and 358 tons per year, respectively (Europe, 2000) (HERA, 2004). Their chemical properties prolong product shelf-life, but are also responsible for their persistence in the environment. The concerns about the release of these chemicals by wastewater treatment plant (WWTP) effluents are largely based on their persistent, bioaccumulative, and endocrine disrupting properties (Simmons et al., 2010; Fernandes et al., 2013; Chen et al., 2011). Those properties include hydrophobicity and selective estrogen receptor modulation (Schreurs et al., 2002).

Despite constant improvements in wastewater treatment technologies, wastewater treatment plant effluents contained HHCB and AHTN up to 2.098 and 0.159 $\mu g \cdot L^{-1}$ respectively in Plymouth (United Kingdom) (Sumner et al., 2010), and up to 13.33 μg HHCB$\cdot L^{-1}$ in Berlin (Heberer, 2002). Consequently, high levels of HHCB and AHTN were found in fish from populated areas. For instance, HHCB and AHTN concentrations reported in crucian carp from Schleswig-Holstein (Germany) were, respectively, 1,551 and 742 $ng \cdot g^{-1}$ wet weight (ww) (Gatermann part one 2002). Yellow perch from Hamilton Harbour (Canada) contained 391 $ng \cdot g^{-1}$ ww HHCB and 96.8 $ng \cdot g^{-1}$ ww AHTN, (O'Toole et al., 2006). Polycyclic musks have been shown to behave like bioaccumulative substances (Klaschka et al., 2013; Gatermann et al., 2002), however, the range of bioconcentration and bioaccumulation factors reported so far is quite large among different species. A similarly large range is seen among the factors normalized per lipid content. This large range of bioaccumulation factors seems to be explained by differences in the rate at which musks are biotransformed and eliminated in fish (Rimkus, 1999). Given these variations, drawing conclusions on the risks and impacts of these chemicals on natural systems can become challenging.

One important Canadian water resource, the North Saskatchewan River, is about 1,300 km long and runs through multiple municipalities, the Edmonton metropolitan area and through the industrial heartland capital region in Alberta. Water from this river is used for drinking, industrial activities, and leisure. In this study, the presence and bioconcentration of musks were characterized near the GBWWTP, the largest wastewater treatment facility in Edmonton, in order to track the fate of musks released in the North Saskatchewan River (NSR). Fathead minnows, a widely used model for environmental studies (Kidd et al., 2014; Jasinska et al., 2015) and a species native to the NSR, were exposed for a period of four weeks

to Gold Bar effluents, which allowed them to accumulate contaminants in an *in vivo* setup. In this project, our two objectives were to (1) characterize the extent of the uptake of HHCB and AHTN in sensitive fish species by analytical determination of HHCB and AHTN in exposed fish; and (2) calculate the bioconcentration factors obtained along a wide concentration gradient.

3.3. Materials and methods

3.3.1. The North Saskatchewan River

The North Saskatchewan River (NSR) flows from west to east, from the Southern Alberta Canadian Rockies in Banff National Park, to Lake Winnipeg mid-Manitoba. Major tributaries at its source consist of the Brazeau, Ram and Clearwater Rivers. The river flow, regulated since 1961, can be controlled by the Brazeau and Bighorn dams. The average flow from April to October is higher (250 $m^3 \cdot s^{-1}$) than during the winter season (121 $m^3 \cdot s^{-1}$). In Alberta, the river drainage basin area is about 55,000 km^2 (for a length of approximately 1,000 km). About one-third of Albertans live in that area and are supplied in water mainly by the North Saskatchewan River. The population living in the drainage basin is mostly located in Edmonton, which is part of the Industrial Heartland and Capital Region (IH-CR, Alberta). The IH-CR, defined by the North Saskatchewan River portion between two long-term river network monitoring stations, Devon and Pakan, supports a growing population and industrial development (AECOM et al., 2011). Such activities consist of urban and infrastructure development, agriculture, coal mining, oil gas abstraction, and power generation. From 2006 to 2011, Edmonton experienced a growth of 12.1%, which is about twice the average Canadian growth for the same period (Statistics Canada, 2012).

From the E.L. Smith water treatment plant (26 km upstream Gold Bar) to the Alberta Capital Region wastewater treatment plant (ACRWWTP) (19 km downstream Gold Bar), the NSR tributaries consist of sewage outfalls releasing sporadically untreated urban runoff in the NSR as well as treated effluents from industries and wastewater treatment facilities. Sewage outfalls contribute mainly to the NSR suspended solid load, in an irregular fashion, as they release runoff mostly with rain events and snow melting occurrences. Most industries located in the greater capital region are involved in oil and gas

activities. One third of the 36 industries in that region are releasing their effluent on a regular basis (AIHA, 2011). Wastewater treatment plant effluents are released continuously in the NSR. Currently, two wastewater treatment plants serve the Edmonton region, the GBWWTP and the Alberta Capital Region WWTP, and they are both releasing treated wastewater on the right bank of the river. Yearly, both WWTPs release a total average of 118,400 ML effluent, and 77% of that number represent Gold Bar's contribution alone.

3.3.2. Gold Bar wastewater facilities

Currently, the two plants treating wastewater in the Edmonton metropolitan area, Gold Bar and the Alberta Capital Region WWTP, respectively release on average 90,800 and 27,600 ML of effluent per year (AECOM et al., 2011). In 2011, the annual flow at Gold Bar reached a total of 102,710 ML, which is the highest Edmonton has seen so far. The Gold Bar Wastewater Treatment Plant (WWTP) (Figure 3.1), built since 1956, now typically treats 300 million litres per day for approximately 800,000 residents (Stantec, 2015). Several upgrades shaped Gold Bar over the years. Biological nutrient removal, UV light disinfection and membrane filtration were respectively added in the 1990s, 2001 and 2005. Raw wastewater entering Gold Bar facilities first undergo pre-treatment, where it is separated from large solid matter by flowing through aerated grit tanks. Solid waste is then forwarded to the Edmonton Waste Management Center. Then, the wastewater undergoes primary treatment, which involves the usage of clarifier tanks from which leftover solids (floaters and sinkers) are skimmed off and scraped, allowing them to be treated separately from the liquids. While the solids go through fermentation and anaerobic digestion, the dissolved constituents pass through secondary treatment in bioreactors where microorganisms multiply and feed on dissolved organic matter and pollutants to break them down. Recent modifications enable microorganisms to remove nutrients from the water, therefore decreasing the load released in the North Saskatchewan River. Following secondary treatment, microorganisms are allowed to form a floc, which then settles to the bottom and permits tertiary treatment. This last treatment consists of UV light disinfection, conducted prior to release of the final effluent in the North Saskatchewan River. Five percent of the effluent will skip UV light

disinfection, as its smallest bacteria are removed from its water with membrane filtration. This filtrated water, or polished effluent, is then distributed to industries.

Technological additions (nutrient removal and UV light treatment) considerably improved nitrogen, phosphorus levels and the bacterial load released with the effluent, which have had positive impacts on the health of the North Saskatchewan River (AECOM et al., 2011). Since the 1980s, environmental health indicators such as biological oxygen demand and diversity of sensitive invertebrate species shifted positively (AECOM et al., 2011). However, despite these implementations, Gold Bar is still the most substantial contributor of nutrients to the North Saskatchewan River. Consequently, algal numbers and biomass were shown to be more abundant on the right bank of the river than on the left bank, which does not receive WWTP effluent from outfall (AECOM et al., 2011).

3.3.3. Experimental design and sample collection

Native fathead minnows (*Pimephales promelas*) were harvested from a pond in the North Saskatchewan River watershed and kept at the University of Alberta aquatic facility during a period of two weeks. They were fed with 1 mm sinking trout pellets, before being caged at six sites upstream and downstream of the GBWWTP. One hundred fish per site were split equally in four Frabill bait buckets and exposed during four weeks from September 13 to October 13, 2011, at reference sites NSR1 and 2, respectively 1.25 and 1.10 km upstream of the effluent release, and at sites NSR3, 4, 5 and 6, which were 0.15, 1, 2.5, and 9.9 km downstream, respectively. The sites downstream were chosen in the plume along the Southbank (i.e. the right bank) of the river (see Figure 3.1). Fish were deployed in Frabill© bait buckets contained within perforated Rubbermaid © containers and fed weekly with the 1mm trout pellets. Following exposure, fish were sacrificed in laboratory with tricaine methanesulfonate. This field work was done by colleagues at University of Alberta and a detailed description can be found in Jasinska et al. (2015). Fathead minnows were sent to the University of Ottawa and were kept at -80°C prior to chemical analysis.

Figure 3.1. Map of the sites in the North Saskatchewan River, Edmonton (Alberta, Canada). The white dot indicates the effluent discharge of Gold Bar WWTP (10977, 50th Street, Edmonton, AB). NSR3 is 150 m downstream, and NSR4, 5 and 6 are respectively 1, 2.5 and 9.9 km downstream. Reference sites NSR1 and 2 are respectively 1.25 and 1.1 km upstream of Gold Bar WWTP. The image was generated by Google Earth Software on 15/02/2015.

3.3.4. Method

The method used for analysis of polycyclic musks HHCB and AHTN in fathead minnows was described in Chapter 2 (2.3.6. Protocol #4). Both male and female fathead minnows were used.

Bioconcentration factors (BCFs) were calculated for each sites following equation (1):

$$BCF = \frac{C_f}{C_w} \quad (1)$$

Where C_f is the mean concentration of musk in fathead minnows (ng·g^{-1} wet weight) and C_w is the mean concentration of musk in water (ng·g^{-1} water at 17°C). Since the diet of fathead minnows was provided during the fish exposure, the result of equation 1 shows the bioconcentration and not bioaccumulation factor, the latter including contamination by dietary uptake. Concentrations in fish were reported here on a wet weight basis, therefore, all bioconcentration factors reported here are calculated on a wet weight basis. Concentrations of musks in water (Table 3.1) used for the calculation of bioconcentration factors are from Jasinska et al. (2015). They were obtained by deployment of semi-permeable membrane devices (SPMDs) along with the mussel and fish cages, over the same 4-week period (September 13 to October 13, 2011). Three SPMDs were mounted per site in perforated stainless steel cages and non-polar contaminants were extracted following the method reported in Helm et al. (2012).

3.3.5. Blanks

Two method blanks were added to each fish extractions, i.e. to approximately six to ten samples. Diatomaceous Earth (Hydromatrix) was used to fill ASE 200 (Accelerated Solvent Extractor) steel extraction vessels. One of the two method blanks per group was spiked with 20 ng of the recovery standard d10-fluoranthene. All extracted method blanks were processed through sample clean-up procedures. All the musks concentrations in fathead minnows presented in this chapter were blank subtracted to account for external contamination. Fragrance-free personal care products were worn during sample processing.

3.3.6. Statistical analysis

One-way Analysis of Variance (ANOVA) was used to identify statistical differences in means between sites, for each musk separately. Homogeneity of variance, tested with Levene's test, was met once logarithmic transformation (equation 2) was applied to the dataset (x), i.e. was applied to concentrations of

musks in fathead minnows (ng·g^{-1} ww). Levene's test is known to be more robust from departures against normality than Barlett's test for homogeneity of variance.

$$y = log_{10}(x + 1) \quad (2)$$

Groups were normally distributed after transformation except for HHCB in fathead minnows (FHM) from NSR2, which failed the p-value criterion of p>0.05 with a value of 0.0028. Despite the violation of one ANOVA assumption, i.e. that the data distribution inside each groups is characterized as normal, ANOVA is known to be generally resistant to deviations from normality (LAERD Statistics, 2016). A possible consequence is a slightly larger type-one error associated with test results, which is estimated to be around 5%. Therefore, differences/similarities between group means revealed by Tukey's post-hoc test following ANOVA were presented as statistically significant. For sample size reasons, ANOVAs were not performed on the data reporting concentrations of musks in water. All statistical analyses were performed with R software (version 3.1.2.) using "lattice", "nlme" and "car" packages. For all analyses, the threshold for significance was chosen to be a p-value of 0.05. Log transformations were also applied to the HHCB to AHTN ratio dataset. Homogeneity of variance was met despite slight departures from normality at NSR1 and 3, which scored p-values of 0.0355 and 0.0129 respectively. Analysis of variance was run on the dataset for the reasons discussed above. Jasinska et al. (2015), which evaluated stress endpoints in fathead minnows from the same sites, also observed a certain variability in their distribution. Therefore, variability may be attributed to the differences in individuals.

3.4. Results and discussion

3.4.1. Reference sites

Mean concentrations of musks in fathead minnows (FHMs) from the reference site NSR1 were higher than NSR2, and were in the low ng·g^{-1} range for both sites (Table 3.1). The frequency of detected musks, after blank corrections, was 100% at NSR1 and 62% at NSR2. Correspondingly, concentrations of musks in water at NSR1 were higher than those at NSR2 which were under the limit of quantitation. Despite this limitation, the presence of musks in water at NSR2 is acknowledged by detectable levels of musks in

FHMs from that same site. Fathead minnows were allowed to bioconcentrate these chemicals, which involved uptake pathways via water, i.e. respiratory and dermal absorption. Therefore, both reference sites NSR1 and 2 were contaminated with HHCB and AHTN. The presence of musks at reference sites was explored further in Chapter 4 (section 4.4.1. Reference sites). Briefly, a combination of an upstream emission of musks to water with volatilization/ deposition processes could have contributed to their presence in water. However, the level of contamination by musks was very low compared to the downstream sites, hence no background correction based on reference sites was applied on musks concentrations in fish and water.

3.4.2. Concentrations of musks in water and fish

A decreasing trend was observed in musk levels in water from NSR3 to 6 (Table 3.1). Means in water from NSR3 to NSR6 went from 381 to 102 $ng \cdot L^{-1}$ for HHCB and from 21.6 to 3.93 $ng \cdot L^{-1}$ for AHTN (Jasinska et al., 2015). The causes of this gradient in musk concentrations in water downstream of Gold Bar are further explored in Chapter 4, where fates of HHCB and AHTN were characterized with a fugacity modelling approach, using QWASI version 3.00 (CEMC, 2005), which calculates contaminant partitioning in described environmental compartments. Levels of musks in water from NSR3 to 6 were comparable with those from other urban waterbodies. First, Bester (2005) reported levels of HHCB and AHTN in several effluents and plumes from the river Rurh (Germany) ranging from 100 to 600 $ng \cdot L^{-1}$ and from 20 to 300 $ng \cdot L^{-1}$ respectively. Those are similar to NSR3 and 4 concentrations, the closest sites to the effluent plume. The same publication characterized water samples taken further from effluent release, nearby the drinking water supply. They contained 60 $ng \cdot L^{-1}$ of HHCB and 10 $ng \cdot L^{-1}$ of AHTN, and were similar to means measured at NSR6, 9.9 km downstream Gold Bar. Surface water mixed with low effluent proportion in Shanghai contained 20 – 93 ng $HHCB \cdot L^{-1}$ and 8 – 20 ng $AHTN \cdot L^{-1}$ (Zhang et al., 2008). Overall, musks in the North Saskatchewan River were generally comparable with concentrations from other urban areas.

Logically, highest concentrations of HHCB and AHTN in exposed fathead minnows (FHMs) were found at NSR3, the closest site to the wastewater treatment plant (WWTP) outfall (Table 3.1.), and are in

the range of 4,300 – 10,900 ng·g^{-1} ww and 179 – 642 ng·g^{-1} ww respectively. These results are comparable to very few other concentrations reported in fish, and the reason why they differ may lie in how this study was designed, i.e., how fish were exposed to these contaminants. Here, FHMs were caged at specific locations and exposed to relatively constant concentrations of musks in water, in contrast to wild caught fish from previous studies that bioaccumulated musks from contaminated river water. Fromme et al. (1999) reported maximum concentrations of HHCB and AHTN of 4,131 and 1,408 ng·g^{-1} fresh weight, respectively, in eels (*Anguilla anguilla*) exposed in water receiving a large proportion of wastewater in Germany. In order to compare these values, it is noteworthy that lipid content in eel was at least twice that of fathead minnows. If these concentrations were to be normalized on a lipid weight basis, HHCB concentrations in FHMs would be much higher than in eel, and AHTN concentrations would be comparable between the two species. Crucian carp (*Carassius carassius*) samples from Germany, with lipid content in the same range of FHMs, were 1,551.4 and 742.9 ng·g^{-1} wet weight (ww) for HHCB and AHTN respectively (Gatermann et al., 2002). These latter values are the closest to our range at NSR3, but differ on the basis of their HHCB to AHTN ratio. The ratio calculated with means reported for Germany was around 2, compared to those from NSR3, which was about 20. Several reasons could explain this difference, such as industry production and usage between areas. Additionally, the geography of the urban waterbody in which fish were exposed, as well as species specific biotransformation pathways, could contribute to the large difference in HHCB to AHTN ratio. Overall, concentrations measured in fathead minnows were either comparable or higher than fish from previous publications.

Table 3.1. Mean concentrations of HHCB and AHTN in fathead minnows and estimated concentrations in water from Semi-Permeable Membrane Devices (SPMDs) in the North Saskatchewan River in Edmonton (AB, CAN). Distances are presented from the source, Gold Bar WWTP effluent, on the river Southbank: negatives are distances upstream of Gold Bar. Standard error (SE) is given. Fathead minnow sample sizes were n=10 for NSR1 and NSR4, n= 12 for NSR2, NSR3 and NSR6 and n=11 for NSR5. For water, n (SPMDs) = 3 at each sites.

Site	Distance	HHCB		AHTN		Recovery
		Fish	Water[1]	Fish	Water[1]	in fish
	km	ng·g^{-1} ww	ng·L^{-1}	ng·g^{-1} ww	ng·L^{-1}	%
NSR1	-1.25	8.7 (0.3)	0.39 (0.18)	0.9 (0.1)	0.11 (0.01)	68 (1)
NSR2	-1.10	6.7 (0.6)	ND	0.5 (0.1)	ND	69 (1)
NSR3	0.15	7,370 (610)	381 (20)	368 (45)	21.6 (1.0)	72 (1)
NSR4	1.00	4,560 (490)	170 (50)	206 (22)	7.27 (1.16)	70 (2)
NSR5	2.50	1,070 (80)	123 (20)	58.8 (3.6)	5.46 (0.42)	66 (2)
NSR6	9.90	894 (46)	102 (10)	39.0 (3.1)	3.93 (0.97)	69 (1)

[1] Jasinska et al. (2015)

With distance from the outfall, i.e. from NSR3 to 5, the concentrations of both polycyclic musks in FHMs decreased significantly (Figure 3.2). Despite the non-significant decrease from NSR5 to 6, the mean and the median of both musks in fish were higher at NSR5 than NSR6. Musk concentrations in FHMs followed the same decreasing trend as observed in water, from the most contaminated sites to the least. Lowest concentrations measured in FHMs at the furthest downstream site (NSR6) were 717 and 22 ng·g^{-1} ww for HHCB and AHTN respectively. Comparable means in yellow perch from Hamilton Harbour, Ontario, were reported to be 391 and 96.8 ng·g^{-1} wet weight (ww), for HHCB and AHTN respectively (O'Toole et al., 2006). In an urban area in Germany, bream (*Abramis brama*) muscle concentrations were 491 and 49.7 ng·g^{-1} ww, for HHCB an AHTN respectively (Rüdel et al., 2006). Overall, HHCB in FHMs from NSR3 and 4 were generally higher than previous data reported in wild caught fish from urban areas, as levels of AHTN were mostly comparable. HHCB and AHTN concentrations in FHMs from NSR5 and 6 were closer to wild caught fish levels.

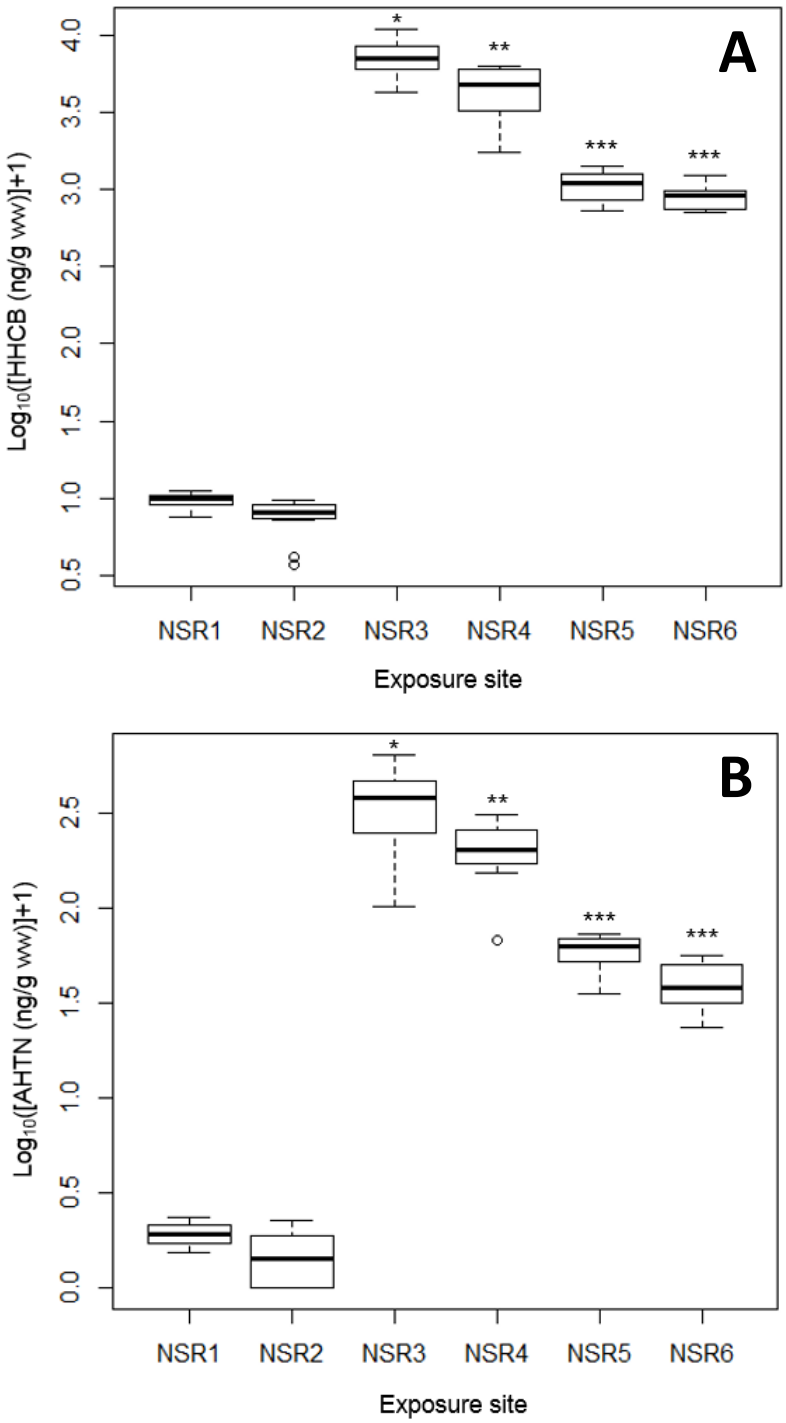

Figure 3.2. Distribution of HHCB (A) and AHTN (B) concentrations ($ng \cdot g^{-1}$ wet weight) accumulated in fathead minnows (*Pimephales promelas*) from September 13 to October 13, 2011, at 6 deployment sites in the North Saskatchewan River, Edmonton (AB, CAN), nearby Gold Bar wastewater treatment plant. Boxes show from top to bottom the upper quartile, median and lower quartile. The whiskers show the maximum and minimum values excluding outliers, the latter represented by the hollow dots. Asterisks acknowledge for statistical differences from reference sites (NSR1 and 2) and other groups tested in a one-way ANOVA. For NSR1 and NSR4, n=10, for NSR2, NSR3 and NSR6, n= 12 and for NSR5, n=11.

3.4.3. Musk ratios and bioconcentration factors

The HHCB to AHTN ratio calculated in water at NSR1 was 4.5 to 6.5 times lower than those downstream of the effluent (Figure 3.3). Since reference site NSR1 was not directly exposed to Gold Bar effluents, the difference in ratio may have been the result of a different source of contamination. Similarly, musk ratio in fathead minnows (FHMs) at NSR1 was significantly lower than NSR3, 4, 5 and 6 (Appendix B).

At NSR3 and 4, HHCB to AHTN ratios in fish were higher than those in water, and at NSR5 and 6, ratios in fish were lower than those in water (Figure 3.3). These two pairs, NSR3-4 and NSR5-6, were also distinguishable when looking at the bioconcentration factors (BCFs) (Table 3.2), as bioconcentration was generally greater for pair A (NSR3-4) than B (NSR5-6), for each individual musk. The separation of these two pairs could be the result of differences in FHM biotransformation of musks caused by the presence of oxidative stress, induced by the wastewater effluent. The following reported information seems to support this hypothesis and is discussed below.

The first indicator of differences in biotransformation between pairs of sites consisted in a comparison of measured to estimated BCFs in aquatic organisms. These estimated BCFs, made on the basis of the log $K_{ow,}$ were 20,700 and 14,000 for HHCB and AHTN, respectively (Rimkus., 1999, citing van de Plassche et al., 1997). The similarity between these numbers and the BCFs calculated at NSR3 and 4 (pair A) is suggesting that bioconcentration at these sites was mostly driven by the compounds affinity for lipids, and that elimination of musks in FHMs was either low or absent. According to Rimkus (1999), a BCF lower than these estimated values would indicate the occurrence of biotransformation and elimination in the targeted aquatic organisms. Therefore, BCFs calculated in FHMs exposed at NSR5 and 6 (pair B) could have been affected by the presence of biotransformation and elimination of musks.

The second indicator of changes in the efficiency of biotransformation of musks due to oxidative stress resides in published half-lives and BCFs for these musks. The half-life of AHTN in bluegill sunfish was previously reported to be shorter (0.8 – 2.1 days) than HHCB (2 – 3 days) (HERA, 2004), at very high levels of exposure (1 to 10 $\mu g \cdot L^{-1}$) in a flow through system. Although the half-lives were not measured as

part of this study, our data seemed to support these measurements, as BCFs for AHTN were lower than HHCB for pair A, i.e. at sites with the highest exposure levels (Table 3.2). The opposite trend, a BCF for AHTN higher than for HHCB, was seen in FHMs from NSR5 and 6 as well as in most reported BCFs from wild caught fishes in urban areas (Gatermann et al., 2002), which were all exposed to lower levels of fragrances.

The third indicator differentiating pair A and B was the difference in FHMs stress levels. Fish from this project were exposed to multiple stressors associated with Gold Bar effluents, such as pharmaceuticals and personal care products (musks), bacterial and nutrient loadings, and were likely to be subjected to a range of stress levels. Jasinska et al. (2015) characterized these levels with several molecular endpoints and found biological indications of stress occurring in FHMs exposed to the most contaminated sites, i.e. pair A. An elevated ratio of oxidized glutathione (GSSG) to total glutathione (TGSH) is caused by the conversion of the reduced form of glutathione to its oxidized form while neutralizing radicals with oxidative potential. Compared to the reference sites, significantly higher ratios of GSSG to TGSH were observed in the liver of fathead minnows from NSR3 and 4 (Jasinska et al., 2015). In addition, oxidative stress occurring at most exposed sites was showed by the induction of the hepatic microsomal enzyme benzo-4-trifluoromethyl-coumarin (BFC). This induction was significant only in fish livers from NSR4 and is an indication of elevated cytochrome P4503A (CYP4503A) activity, also involved in drug metabolism. As FHMs from NSR3 and 4 (pair A) showed evidence of stress, FHMs from NSR5 and 6 (pair B) showed biomarker levels closer to those exposed at reference sites (Jasinska et al., 2015).

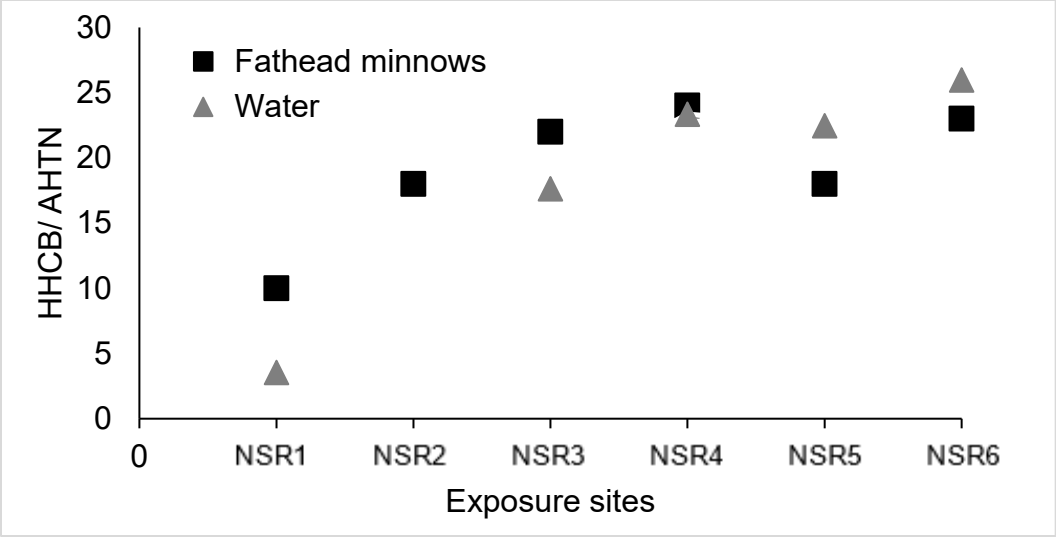

Figure 3.3. Mean of HHCB to AHTN concentration ratios (no units) in water and in exposed fathead minnows at 6 sites in the North Saskatchewan River, Edmonton. For NSR1 and NSR4, n=10, for NSR2, NSR3 and NSR6, n= 12 and for NSR5, n=11.

Table 3.2. Bioconcentration factors calculated as the mean concentration of musk found in fathead minnows in $ng \cdot g^{-1}$ wet weight divided by the concentration in water in $ng \cdot g^{-1}$, converted from $ng \cdot L^{-1}$ with the density of water at 16.9°C. Log10 of the bioconcentration factor is in parenthesis. For NSR1, 2, 3, 4, 5 and 6, the mean musk concentrations were calculated out of n=15, 18, 16, 14, 18 and 19 fish samples respectively. In water, the mean concentrations for NSR1 to 5, were calculated with n=3 semi-permeable membrane devices (SPMDs) and for NSR6, n=2.

Site	HHCB	AHTN
NSR1	22,000 (4.3)	8,900 (3.9)
NSR2	ND	ND
NSR3	18,600 (4.3)	14,900 (4.2)
NSR4	24,500 (4.4)	22,300 (4.3)
NSR5	7,820 (3.9)	12,800 (4.1)
NSR6	6,670 (3.8)	11,100 (4.0)

Overall, the bioconcentration factors (BCFs) obtained with our exposure experiment were quite high compared to BCFs reported *in situ* from other studies. BCF values from other previous publications, reporting wet weight based BCFs in fish species, were generally one to two orders of magnitude lower than values reported here. For example, BCFs reported by Fromme et al. (2001) ranged between 201 – 1,561 for HHCB and 250 – 1,791 for AHTN. So far, bioaccumulation factors in aquatic biota were more often reported than bioconcentration factors, but were overall in the same range. Bioaccumulation factors

reported by Gatermann et al. (2002) ranged between 20 – 620 for HHCB and 40 – 670 for AHTN for various aquatic species, such as Rudd (*Scardinus erythrophtalmus*), Tench (*Tinca tinca),* Crucian carp (*Carassius carassius*), Eel (*Anguila anguila*), and Zebra mussel (*Dreissena polymorpha*). To our knowledge, we are the first to report BCF values for polycyclic musks in fathead minnows. The difference between high BCFs from this work and BCFs reported in wild caught fish could be influenced by our study design. Wild caught fish were allowed to spend time in water contaminated to different degrees, whereas our fish were contained in cages suspended in the river, so the overall level of exposure via water by wild caught fish was probably lower than fathead minnows exposed even at our furthest site downstream. As previously discussed, fish under lower stress and exposed to relatively lower levels of polycyclic musks seem to favor HHCB biotransformation, which could be part of the reason why lower BCFs for HHCB were reported in previous publications. Also, wet weight based BCF values are dependent on organism lipid content, which varies from one species to another. Additionally, foreign compounds biotransformation of reported fish species could have been normally more efficient than biotransformation in fathead minnows, which could explain why we had higher BCF values.

3.4.4. Implications of bioconcentration for endocrine disruption in fish

Concentrations of HHCB in female FHMs exposed at the two most contaminated sites ranged from 2.77 to 10.9 $\mu g \cdot g^{-1}$ and were mainly above the half maximal vitellogenin (VTG) inhibitory concentration (IC50) reported by Simmons et al. (2010) in rainbow trout, which was 3.64 $\mu g \cdot g^{-1}$. In rainbow trout, this toxicity threshold corresponded to antagonistic activity toward ERα by substrate competition at the binding sites. That IC50 translated into a 10% decrease in VTG concentrations when compared to control fish.

In male medaka fish (*Oryzias latipes*), HHCB and AHTN had agonistic behavior by induction of ERα associated mRNA and hepatic vitellogenin at concentrations in water of 500 µg musk$\cdot L^{-1}$ (Yamauchi et al. 2008). Exposure to 5 $\mu g \cdot L^{-1}$ HHCB or AHTN, the lowest level tested by Yamauchi et al. (2008), did not induce changes in these biomarkers. Highest exposure levels in this study (0.38 µg HHCB$\cdot L^{-1}$) were about 13 times lower than 5 $\mu g \cdot L^{-1}$, therefore, the likelihood for induction of vitellogenin in male FHMs

caused by musks is probably quite low. Consequently, the significantly elevated vitellogenin levels observed in male FHMs from NSR3 and 4 (Jasinska et al. 2015) maybe due to the presence of other endocrine disruptors in the Gold Bar effluents. HHCB decreased the activity of enzymes (Cyp17 and Cyp11 β) catalyzing testosterone precursors in the European sea bass (*Dicentrarchus labrax*) injected a dose of 50 $\mu g \cdot g^{-1}$ (Fernandes et al., 2013). After 24 hours, HHCB inhibited about 30% of the Cyp17 activity, and 96 hours post injection, 30% of the Cyp11β activity. Activity reduction of Cyp17 and Cyp11β enzymes by Fernandes et al. (2013) occurred at levels at least 5 times greater than those reported in FHMs from this study (10.9 $\mu g \cdot g^{-1}$ HHCB). Without further information, a statement cannot be made regarding disruption of testosterone synthesis pathways in male FHMs, but we can express with a certain level of confidence that HHCB was not a substantial threat to the male reproductive system. At NSR5 and 6, concentrations of musks in FHMs were lower than toxicity thresholds. Also, concentrations of AHTN are too low to cause any estrogenic effects.

3.5. Conclusion

HHCB and AHTN concentrations were determined in fathead minnows that were exposed to a contaminated location in Edmonton (CA), downstream of the Gold Bar wastewater treatment plant effluents. Those concentrations were much higher than those previously reported in urban locations, possibly because our study design used caged fish held in the wastewater effluent. This design allowed the calculation of bioconcentration factors in fish subjected to different concentrations of musks as well as different oxidative stress levels. The calculation of the HHCB to AHTN ratio of musks in the North Saskatchewan River as well as in fish, with the BCFs, suggested that stressed fathead minnows were not able to biotransform and eliminate these fragrances as efficiently as fish exposed to lower levels. Since the concentrations of musks in fathead minnows (males and females) exposed at the most contaminated sites were about 3 times higher than effect doses reported for female rainbow trout, the vitellogenin levels of the female portion of FHMs exposed to the most contaminated sites in the NSR could have been affected by synthetic musks.

Chapter 4

4. Fate of synthetic musk fragrances HHCB and AHTN in the North Saskatchewan River, Edmonton

4.1. Abstract

The fate of HHCB and AHTN, fragrances both released in the North Saskatchewan River (NSR) by Gold Bar wastewater treatment plant (GBWWTP, Edmonton), was assessed with the Quantitative Water Air Sediment Interaction (QWASI) Model. The section of the NSR used was divided in 6 compartments according to effluent mixing. The input of chemical and environmental properties in the fugacity model QWASI successfully explained distributions of HHCB and AHTN in the North Saskatchewan River near Edmonton. The largest fluxes of the musks were by water advection and sedimentation, and amounted to about 99% of losses to the system. Predicted concentrations in different environmental media were in the same range as reported data on musks from urban areas except for sediments, which were possibly overestimated. The model fit to measured data was calculated and resulted in a slight overestimation of musks concentrations in water, from 0.2 to 34% for most compartments. A limitation of the model was shown by a discrepancy between predicted and measured concentrations in water observed near a refinery effluent outfall.

4.2. Introduction

Pharmaceutical, personal care and household cleaning products such as shampoo, deodorant, soap and detergent are known sources of polycyclic musk fragrances to urban waterbodies through wastewater treatment plant (WWTP) effluents. Among polycyclic musks, Galaxolide (HHCB) and Tonalide (AHTN) production represent 95% of the European Union (EU) market, with levels of 1,427 and 358 tons produced per year in Europe in 2000 (HERA, 2004). HHCB and AHTN are hydrophobic, persistent, bioaccumulative (Boethling, 2011) and ubiquitous in environmental compartments in urban areas, such as water and sediments (Zhang et al., 2008), fish (O'Toole et al., 2006) and in/outdoor air from urban areas (Fromme et al., 2004; Peck et al., 2006). Concern about the presence of musks in the environment is due to both their chemical and toxic properties, as HHCB and AHTN were reported to act as endocrine disruptors (Simmons

et al., 2010) as well as environmental stressors (An et al., 2009; Chen et al., 2011; Wollenberger et al., 2003). This study aimed to characterize the extent of their presence in a contaminated area, a section of the North Saskatchewan River (NSR) passing through the Edmonton metropolitan area. Currently, two wastewater treatment plants release their effluents in the Edmonton section of the NSR. These are Gold Bar and the Alberta Capital Region WWTP (19 km downstream), which respectively release on average $0.908 \cdot 10^8$ and $0.276 \cdot 10^8$ m^3 effluent per year. In 2011, the Gold Bar's annual flow reached a total of $1.0271 \cdot 10^8$ m^3, which is the highest Edmonton has seen so far (EPCOR, 2015). This peak was probably partially due to population growth. From 2006 to 2011, Edmonton experienced a growth of 12.1 %, compared to the Canadian average growth of 5.9% during the same period (Statistics Canada, 2012), with a population of 1,159,869 habitants in 2011. Furthermore, population growth could lead to increased concentrations of fragrances in the NSR, due to the presence of musks in a variety of domestic products. In order to characterize the presence of musks in the North Saskatchewan River, the fate of these chemicals was modeled with Quantitative Water Air Sediment Interaction software (CEMC, 2005), from their release (GBWWTP) up to 11 km downstream. This chapter focuses on two objectives (1) to determine which processes drove the loss of HHCB and AHTN in the North Saskatchewan River, i.e. volatilization, degradation, and/ or sedimentation, and (2) to evaluate the partition model by comparing predicted values to measured data. A better understanding of synthetic fragrances behaviour in waterbodies such as the NSR should provide more tools in the assessment of anthropogenic impacts of population growth in the Edmonton metropolitan region.

4.3. Methodology

QWASI software processes the calculations involved in fugacity modelling at different levels, and each level uses specific assumptions. In Level II, the one used for this project, the software was given parameters (Table 4.2.) characterizing the chemical compounds and phases in a given compartment, and calculated the chemical partitioning in each phase. Level II is a steady state model, with the advective chemical input (inflow and emission) being equal to the total output (reaction and outflow) in the

compartment. To determine the fate of musks in the North Saskatchewan River, we sectioned the river in several compartments according to Mackay et al., (1983), which involved dividing the river into a series of volumes, each of which was treated as being homogenous or well-mixed in both water and sediment. This approach views the river as a series of connected water bodies, each of which can be treated using the QWASI model. The QWASI modelling software version 3.00 (CEMC, 2005) was used to treat each compartment to assess musk partitioning. The North Saskatchewan River was divided in six compartments, from A to F, around GBWWTP (Figure 4.1.). Division of the compartments considered two factors: (a) the effluent mixing and (b) water sampling site locations NSR1 to 6 (Table 3.1, Chapter 3). Google Earth Pro was used for delineation and area measurements, as well as for the maps presented in this chapter.

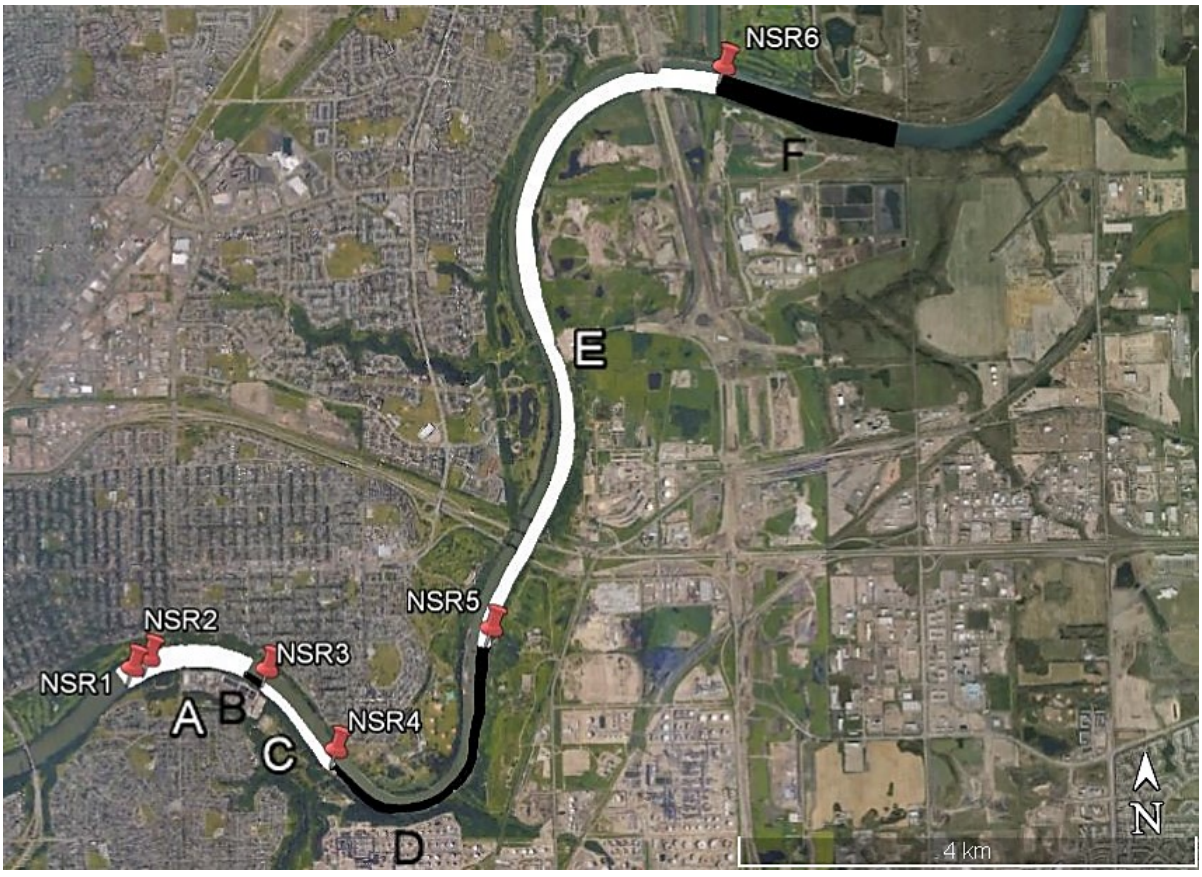

Figure 4.1. Delineation of compartments used for fate modelling of HHCB and AHTN in the North Saskatchewan River, represented by the letters A to F. Sites are indicated with pins. Wastewater effluent is released at compartment B, where Gold Bar WWTP is located.

First, physical mixing of Gold Bar effluent with ambient river water from the NSR was considered in the delineation of compartments. The effluent discharge, containing musks, does not mix evenly with ambient water once released in the NSR (Pilechi et al., 2012). Therefore, to generate the series of well mixed water volumes (or compartments) needed for the model, the way the effluent mixes in the NSR was taken into account. The Gold Bar effluent mixing in the North Saskatchewan River was described in Pilechi et al. (2012), which was cited by the Alberta Environment and Sustainable Resource Development (AESRD) report, the latter kindly provided by EPCOR Water Canada (AECOM et al., 2011). This information was used to set the compartment perimeters. From the outfall to the end cross section 11.6 km downstream, the compartment width gradually increased from 50 meters from the right bank up to the full cross section of the river at 11.6 km (Appendix C). The cross section at NSR1, upstream Gold Bar, was assumed to be well mixed compared to the cross section at outfall: thus, the full magnitude of the river width (or cross-section) was used to delineate compartment A. Secondly, site locations NSR1 to 6 were used in the delineation of compartments with the musk concentrations in water quantified at these sites. The concentrations of musks in water at sites NSR1 to 6 were determined with Semi-Permeable Membrane Devices and were previously reported in Jasinska et al. (2015). HHCB and AHTN were not detected at NSR2, and as a consequence, compartment A starts at NSR1 and stops before the effluent, which includes NSR2.

The concentrations of musks in air input in the model (Table 4.1) were assumed to be steady and at equilibrium with water. They were calculated with respect to the measured water concentrations in each compartment (Table 4.1), according to Mackay (1991) equation for fugacity level one models as shown by equation 1:

$$C_a = \frac{C_w \cdot H}{R \cdot T} \quad (1)$$

Where C_a is the concentration of musk in air in $mol \cdot m^{-3}$, C_w is the concentration of musk in water in $mol \cdot m^{-3}$, H is the Henry's law constant in $Pa \cdot m^3 \cdot mol^{-1}$, R is the gas constant in $m^3 \cdot Pa \cdot K^{-1} \cdot mol^{-1}$ and T is the temperature in Kelvins (K). Concentrations of musks in inflow water used for most compartment models

were reported at 6 sites (NSR1 to 6) in Chapter 3 and are presented in Table 4.1. When measured inflow concentrations were not available, model predicted concentrations in outflow from the preceding compartment were used instead. For example, no data were available for compartment B inflow concentrations, therefore, compartment A predicted musk concentration in outflow water was used as inflow for B. The direct discharge in the water, or emission parameter, was determined by trial and error until the predicted concentration matched the measured concentration of musk at NSR3.

Table 4.1. Emission and inflow parameters input in QWASI model software for fate prediction of HHCB and AHTN in the North Saskatchewan River, Edmonton (AB, CAN).

Musk	Parameter	Compartment						Units
		A	B	C	D	E	F	
HHCB	**Chemical Concentration in Inflow Water**	0.39	0.38	382	170	123	102	**ng·L^{-1}**
	Chemical Concentration in Air[1]	6.01	5920	5920	2630	1900	1580	**ng·m^{-3}**
AHTN	**Chemical Concentration in Inflow Water**	0.11	0.11	21.6	7.27	5.46	3.93	**ng·L^{-1}**
	Chemical Concentration in Air[1]	1.72	338	338	113	85.0	61.2	**ng·m^{-3}**

[1] Peck et al., 2004

Most of the chemical properties used in the model were presented in Table 1.1 (Chapter 1), except for AHTN half-lives in water and in sediment, which, to our knowledge have not been reported yet. To fill this gap, HHCB half-lives were used for AHTN in the QWASI model, as HHCB and AHTN have similar chemical structures and properties (38 and 1,896 h for water and sediment, respectively). The ambient temperature for the model was input as the mean in water during the sampling period of September 13 to October 13, 2011, which was 13.1ºC.

The volume of each compartment (Table 4.2) was calculated with the average depth of the river according to Pilechi et al. (2012) at different cross sections downstream Gold Bar:

$$V = Depth * Area \quad (2)$$

The city of Edmonton, during the period of September – October, saw the least precipitation in 2011, the period in which the field data collection took place. However, the input for the rain rate parameter (Table 4.2) in QWASI had to be expressed in $m \cdot year^{-1}$. In order to appropriately represent the fate of HHCB and AHTN, the twelve months extrapolated mean of September and October precipitations, 0.084 $m \cdot year^{-1}$, was preferred against the total precipitation for the year of 2011, 0.466 $m \cdot year^{-1}$ (Government of Canada, 2015). This influenced the deposition rate of contaminants, lowering the transfer rate of chemical from air to water. All other environmentally relevant inputs, either previously reported or estimated, are presented in Table 4.2 with their corresponding references.

One of the strengths of this model is its adaptability to different chemicals and environment types, due to a high number of variables. Also, the outputs of such a model are easily understandable (reaction time, residence time, concentrations). However, limitations of the model can occur with the geography of the site, the availability of the data that is characterizing both the chemical compound and the environment, and the division of the different compartments in the waterbody.

Table 4.2. Environmental parameters describing six compartments in the North Saskatchewan River, Edmonton (AB, CAN), required by QWASI for the purpose of fugacity modelling during the mid-September to mid-October 2011 period.

Environmental Parameter	Compartment						Units
	A	B	C	D	E	F	
Water surface area	208,045	9,633	62,406	159,111	733,160	322,558	m^2
Water volume	321,638	14,893	96,480	245,986	919,383	361,265	m^3
Sediment active layer depth[1]	0.025	0.035	0.035	0.035	0.030	0.030	m
Concentration of solids							
in Water column[2]	2	10	7	5	4	4	$mg \cdot L^{-1}$
in Inflow water	2	10	10	6	5	4	$mg \cdot L^{-1}$
of Aerosols in air	10	10	10	10	10	10	$\mu g \cdot m^{-3}$
in Sediment	0.3	0.9	0.9	1	0.8	0.8	$m^3 \cdot m^{-3}$
Density of solids							
in Water column[1]	2,600	2,600	2,600	2,600	2,600	2,600	$kg \cdot m^{-3}$
of Sediment[1]	2,600	2,600	2,600	2,600	2,600	2,600	$kg \cdot m^{-3}$
of Aerosols in air[1]	1,500	1,500	1,500	1,500	1,500	1,500	$kg \cdot m^{-3}$
OC fraction of solids							
in Water column[2]	0.2	0.9	0.5	0.5	0.2	0.2	N/A
in Sediment	0.2	0.9	0.4	0.4	0.2	0.2	N/A
in Inflow water	0.2	0.9	0.3	0.3	0.3	0.3	N/A
in Resuspended sediment[1]	0.03	0.05	0.03	0.03	0.03	0.03	N/A
River water inflow[3]	432,000	432,000	432,000	432,000	432,000	432,000	$m^3 \cdot h^{-1}$
Water outflow rate[3]	432,000	432,000	432,000	432,000	432,000	432,000	$m^3 \cdot h^{-1}$
Deposition rate of solids[1]	5	6	5	5	5	5	$g \cdot m^{-2}$ day
Burial rate of solids	1	1	2	1	1	1	$g \cdot m^{-2}$ day
Resuspension rate of solids	1	1	1	1	1	1	$g \cdot m^{-2}$ day
Atmospheric deposition							
Aerosol dry deposition velocity	7.2	7.2	7.2	7.2	7.2	7.2	$m \cdot h^{-1}$
Scavenging ratio (vol air/ vol rain)[1]	200,000	200,000	200,000	200,000	200,000	200,000	N/A
Rain rate	0.084	0.084	0.084	0.084	0.084	0.084	$m \cdot year^{-1}$
Volatilization MTC (air side)[1]	0.025	0.025	0.025	0.025	0.025	0.025	$m \cdot h^{-1}$
Volatilization MTC (water side)[1]	0.025	0.025	0.025	0.025	0.025	0.025	$m \cdot h^{-1}$
Sediment-water diffusion MTC[1]	0.08	0.08	0.08	0.08	0.08	0.08	$m \cdot h^{-1}$

[1] Default environmental parameters, QWASI software
[2] Köster et al., 2014
[3] AECOM et al., 2011

4.4. Results and discussion

4.4.1. Reference sites

Compartment A, upstream Gold Bar effluent, was only slightly contaminated by musks, as HHCB and AHTN were detected in water at NSR1 at concentrations of 0.39 $ng \cdot L^{-1}$ and 0.11 $ng \cdot L^{-1}$ respectively. At NSR2, both musks were under the limit of detection, but were presumably present in water due to detectable levels of musks in fathead minnows exposed at that site (see Chapter 3, Table 3.1). Sources of musks at reference sites located upstream of Gold Bar effluents are likely to come from a combination of small contributions such as deposition and upstream effluents. First, deposition could have contributed to musk contamination of the reference sites. Volatilized musks from the air above Gold Bar effluents could have been deposited at NSR1 and 2, respectively 1.25 and 1.1 km upstream. Although musk atmospheric half-lives are not sufficient to support long range transportation, they might allow transportation on short distances such as a few kilometers. The half-lives were reported to be 3.4 hours and 7.3 hours for HHCB and AHTN, respectively (Aschmann et al., 2001). As AHTN was found to be more persistent than HHCB when volatilized, the HHCB to AHTN ratio in water at the deposition site would likely be lower at than the one in water at the volatilization site. In our case, the calculated HHCB to AHTN ratio in water at the possible deposition site (NSR1) was 4.5 times lower than at volatilization site (NSR3) (Figure 3.3, Chapter 3). This difference in ratios from both sites could be an indication that volatilization and deposition processes are responsible for contamination at site NSR1. Given that, compartment A might be an exception to the equilibrium assumption between air and water concentrations (equation 1) made for this model. To test this scenario, an additional QWASI model was executed, where the concentrations of HHCB and AHTN in air above compartment A (NSR1 and 2) were the same as the ones in air above compartment B (NSR3), for assessing the maximum contribution scenario of deposition in compartment A. Concentrations of HHCB and AHTN in air above NSR3, calculated under the assumption of equilibrium for modelling purposes (see section 4.3. Methodology), were 5.9 and 0.34 $\mu g \cdot L^{-1}$ respectively. Given that these concentrations of musks in air would be the only source of musks of compartment A, they would partition in the river water at concentrations of 0.087 and 0.0045 $ng \cdot L^{-1}$, for HHCB and AHTN respectively. For

HHCB and AHTN respectively, this was 22.3 and 4.1% of the actual measured concentration in water at NSR1 (Table 4.1). Therefore, deposition processes alone are only explaining 22.3 and 4.1% of HHCB and AHTN measured concentrations at reference site NSR1. Secondly, upstream effluents that could have contributed to musks at reference sites are mostly combined sewer outfalls (CSOs) and water treatment plants (WTP), like the Rossdale WTP, which treats North Saskatchewan River water for distribution to the city of Edmonton (AECOM et al., 2011). Combined sewer outfalls are occasionally releasing untreated urban runoff in the North Saskatchewan River, which could contain musks. Contaminated runoff discharging upstream the reference site could have contributed to the musks concentration measured at NSR1. Additionally, the Rossdale WTP, located 9 km upstream of Gold Bar, releases industrial discharges on the right bank of the North Saskatchewan River when necessary. It is possible that Rossdale effluents released in the river contained musks, but since this facility does not treat wastewater from the city, the concentration of musks in the WTP effluent would be much lower than effluent from wastewater treatment plants.

4.4.2. WWTP discharge

In compartment B, the model was used to estimate the direct discharge of musks needed to generate the observed concentrations in water. They were 1,445 and 85 $kg \cdot year^{-1}$, for HHCB and AHTN respectively. In order to compare these discharges, the corresponding concentrations of musks in the effluent were calculated according to the effluent total volume in 2011 (EPCOR, 2015). The calculated effluent concentrations of HHCB and AHTN were 14.1 and 0.828 $\mu g \cdot L^{-1}$, respectively. These numbers are comparable to those in Sumner et al. (2010), who reported concentrations in effluents from Plymouth (United Kingdom). For HHCB, they found concentrations in the range of 0.987 – 2.098 $\mu g \cdot L^{-1}$, and for AHTN, in the range of 0.055 – 0.159 $\mu g \cdot L^{-1}$. HHCB discharge from Gold Bar effluent was closer to what was reported by Heberer (2002) in a published review, who reported mean values from 30 water sampling locations in Berlin, a densely populated area. For HHCB and AHTN, respectively, mean values were 7.58 and 2.64 $\mu g \cdot L^{-1}$, with a maximum of 13.33 $\mu g \cdot L^{-1}$ HHCB recorded at effluent. The ratio of HHCB to AHTN

in effluents from Berlin was six times lower than the ratio calculated with predicted Gold Bar effluent values. The difference in these ratios can be attributed to the difference in synthetic fragrance production and consumption from these two areas, i.e. the usage per capita, as well as the population density, the WWTP influent capacity and the treatment applied. Also, generally speaking, the ratios of HHCB to AHTN reported in various environmental compartments has increased over the last few years as their consumption changed, so a lower ratio in effluents from 2002 compared to 2011 is expected. Appendix D shows compiled data with this tendency in biota from different locations over the years. Briefly, both HHCB and AHTN predicted concentrations in Gold Bar discharge were probably realistic estimations of the exact values.

The model predicted concentrations of musks in sediment much greater than those reported from other studies focusing on effluent outfall locations. For example, sediment from the UK, receiving effluents with 987, 2,098 and 1,598 $ng \cdot L^{-1}$ HHCB showed concentrations of 15, 16 and 16 $ng \cdot g^{-1}$ dry weight, respectively (Sumner, 2010). According to our model in compartment B (outfall), the effluent discharge contained 14,100 $ng \cdot L^{-1}$ HHCB and sediment concentration was 492 $ng \cdot g^{-1}$ dw (dry weight). Despite the comparable HHCB concentrations in UK effluents to our data, measured sediment concentrations in the UK are lower than our predicted value in compartment B sediment. Concentrations of AHTN in discharge and sediment in compartment B showed the same gap when compared with reported data in Sumner (2010). Also, predicted sediment concentrations of musks in compartment C, D, E and F were very high. This comparison between the previous numbers are suggesting the occurrence of a faster degradation in sediment than what was assumed in our model, in which HHCB had a half-life of 79 days (HERA, 2004). This difference could also be due to environmental factors, such as organic content of sediment and particulates, suspended sediment load, and other features that had to be estimated in our model. In order to improve our understanding of this discrepancy, the possibility of 79 days being an overestimation of half-lives was assessed with additional QWASI runs, in which lower half-lives were tested in compartment C. The values entered for the half-lives parameters of musks were modified in order to obtain values of musk concentrations in the range reported in the literature for outfall sediments, which were 11 – 17, 7.0 – 78.0 and <0.5 – 56 $ng \cdot g^{-1}$ dw for HHCB and 2 – 10, 2.0 – 21.0 and 23 – 90 $ng \cdot g^{-1}$ dw for AHTN, in Sumner et

al. (2010), Zhang et al. (2008) and Kronimus et al. (2004) respectively. For a HHCB half-life of 4.2 days, concentration obtained in sediment was 35 $ng \cdot g^{-1}$ dw and for a AHTN half-life of 42 days, 22 $ng \cdot g^{-1}$ dw was obtained for AHTN. These differences between the half-life used in this model (79 days) and the ones obtained by matching sediment concentrations values (4.2 and 42 days) are leading us to think more work has to be conducted on the determination of half-lives of musks in sediment. Very few publications report half-lives of musks in different environmental media. Although publications reported degradation of musks in sludge and amended soils (Chen et al., 2014; Chen et al., 2009; Balk et al., 1999a), half-lives of musks in sediment are not as accessible (Envirogen, 1998) and need to be better documented. Although the half-lives may have been overestimated in this model for sediments, factors such as bacterial biotransformation could be responsible for differences between predicted and reported concentrations in sediments near WWTP effluents.

4.4.3. Fugacity and fate

According to the QWASI model, HHCB and AHTN have very similar behaviour in compartments B to F, once released in the North Saskatchewan River. For each individual musk, transfers characterizing their behaviour in a given compartment (except for compartment A) are similar from one compartment to the other: the highest musk transfer rates are outflow, followed by sedimentation, reaction (transformation) in water and lastly, by volatilization (Figure 4.2 and 4.3).

The highest musk transfer rate was in the outflow. For HHCB in each compartment, outflow rate represented 86.9 to 99.8% of its corresponding inflow rate. For AHTN, outflow represented a proportion of 86.5 to 99.8%. Therefore, according to our model, outflow was the main driver of polycyclic musks fate in the North Saskatchewan River (NSR). The remaining fractions were lost by sedimentation, reaction and volatilization.

For compartment B to E, loss of musks by sedimentation was responsible for up to 10.0% loss for HHCB and up to 10.2% for AHTN. In the North Saskatchewan River, the loss of musks by sedimentation was mainly led by particulate matter deposition and reaction in sediments. Suspended particulate matter

often transports hydrophobic contaminants such as HHCB and AHTN, as they tend to partition preferably to the organic carbon fraction contained to the particulate matter. Then, suspended particulates eventually settle to the bottom by gravity. After sedimentation, loss by reaction in water was the second most important loss process in determination of fate. Loss by reaction represented up to 3.37% of transfers for HHCB and up to 3.35% for AHTN. Finally, the model estimated very little loss by volatilization. The contribution of loss by volatilization was in the range of $6.4 \cdot 10^{-5}$ – $1.1 \cdot 10^{-2}$% for HHCB and $1.03 \cdot 10^{-4}$ – $1.5 \cdot 10^{-2}$% for AHTN.

At the outflow of compartment F, 11.6 km downstream of Gold Bar effluent, HHCB and AHTN predicted concentrations in water were respectively of 95.6 and 3.7 $ng \cdot L^{-1}$. Further modelling could be done to predict musk concentrations in water past compartment F. The presence of ACRWWTP would have to be considered as a source. As mentioned previously, 19 km downstream of Gold Bar sits the Alberta Capital Region Wastewater Treatment Plant, which treats on average 27,600 ML per year (AECOM et al., 2011).

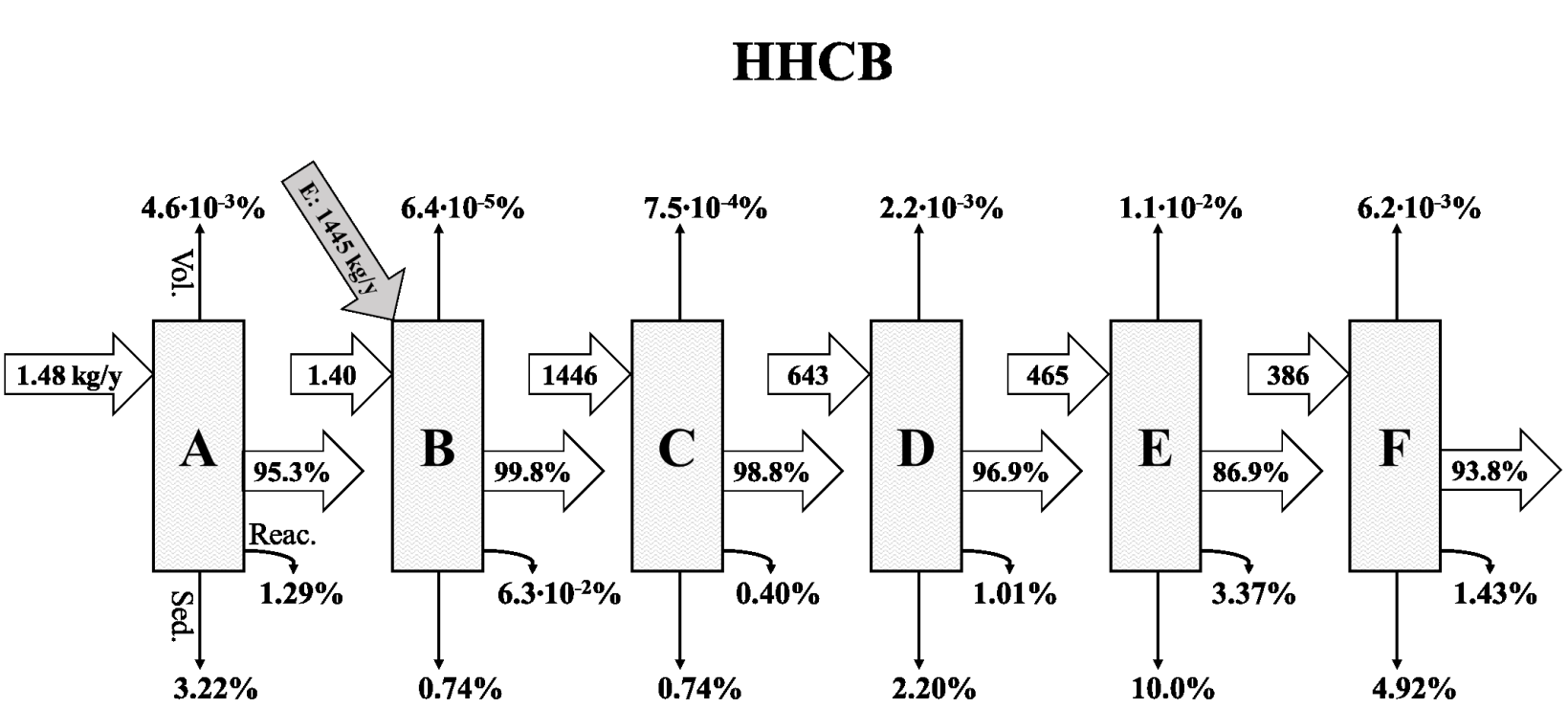

Figure 4.2. Emission (E) and flows characterizing HHCB's fate in 6 water compartments in the North Saskatchewan River, surrounding Gold Bar WWTP (Edmonton, AB). Gold Bar emission (kg HHCB·y^{-1}) is represented by the grey arrow at compartment B. Flows include water inflow, outflow, volatilization, sedimentation and loss by reaction in water. Water inflows, (kg HHCB·y^{-1}) and outflows (%) are represented by the thick white arrows. Loss by volatilization (%) and sedimentation (%) are represented by the thin straight arrows. Loss by reaction in water (%) is represented by the thin curvy arrows. The percentages were calculated by dividing the specific flow rate, expressed in kg HHCB·y^{-1}, by the total of the emission and inflow rate for each compartment, also expressed in kg HHCB·y^{-1}, and by multiplying the result of this ratio by 100%. The inflow rates were calculated by multiplying the measured concentrations of musk in water (kg·m^3) (Table 4.1) with the river water flow rate (m^3·y^{-1}).

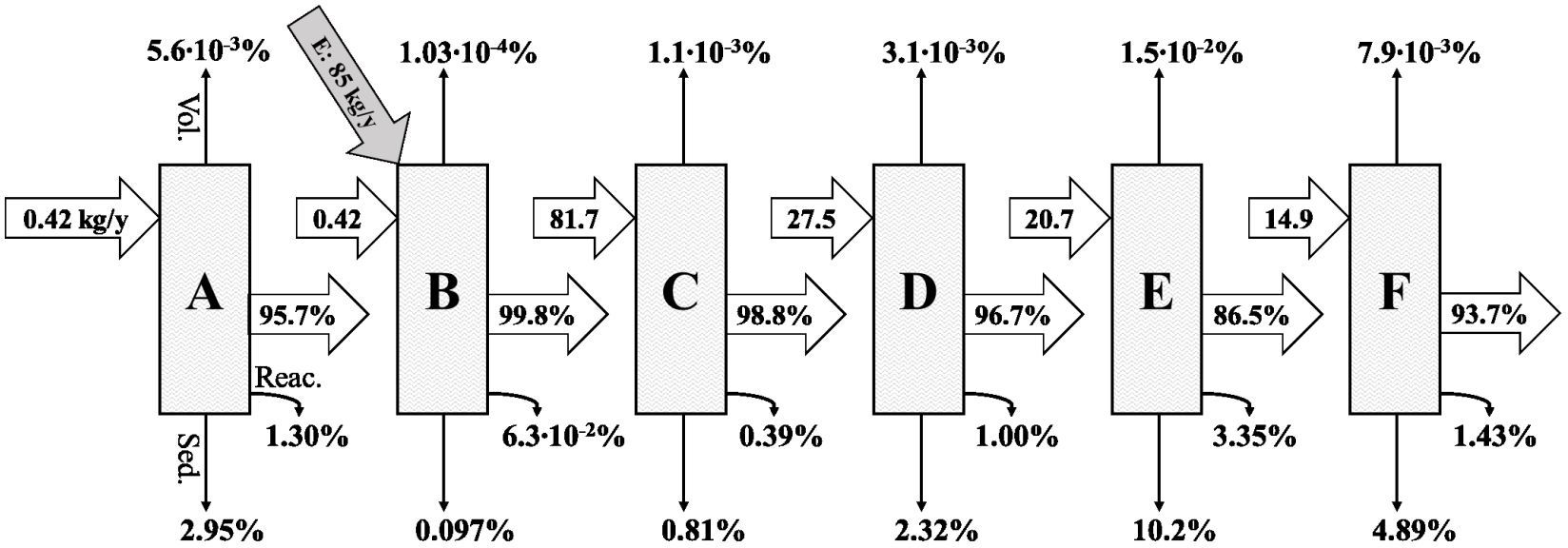

Figure 4.3. Emissions (E) and flows characterizing AHTN's fate in 6 water compartments in the North Saskatchewan River, surrounding Gold Bar WWTP (Edmonton, AB). Gold Bar emission (kg AHTN $\cdot y^{-1}$) is represented by the grey arrow at compartment B. Flows include water inflow, outflow, volatilization, sedimentation and loss by reaction in water. Water inflows, (kg AHTN $\cdot y^{-1}$) and outflows (%) are represented by the thick white arrows. Loss by volatilization (%) and sedimentation (%) are represented by the thin straight arrows. Loss by reaction in water (%) is represented by the thin curvy arrows. The percentages were calculated by dividing the specific flow rate, expressed in kg AHTN $\cdot y^{-1}$, by the total of the emission and inflow rate for each compartment, also expressed in kg AHTN $\cdot y^{-1}$, and by multiplying the result of this ratio by 100%. The inflow rates were calculated by multiplying the measured concentrations of musk in water ($kg \cdot m^3$) (Table 4.1) with the river water flow rate ($m^3 \cdot y^{-1}$).

4.4.4. Predicted VS measured values

The model was able to explain most of HHCB and AHTN behavior in environmental compartments, however, a discrepancy was observed between predicted and measured data for both musks in compartment C: the model scored a predicted value of 378 $ng \cdot L^{-1}$ compared to a measured outflow value of 170 ± 45 $ng \cdot L^{-1}$ for HHCB, and respective values for AHTN were 21.3 and 7.27 $ng \cdot L^{-1}$ (Figure 4.4). The predicted values were 222% and 293% of their measured values for HHCB and AHTN respectively. A possible cause of this discrepancy could be the industrial effluent from the Imperial Oil Strathcona Refinery, which is being released at about 262 $m^3 \cdot h^{-1}$ (AECOM et al., 2011). This effluent is probably not likely enriched with musks, due to its nature. About one kilometer downstream of Gold Bar, the refinery effluent is located right by NSR4 (Figure 4.5). The particular shape of the junction between this tributary and the North Saskatchewan River seems to release effluent in all directions, due to its large Y figure. Despite the refinery effluent outfall located a few meters downstream NSR4, it may have contributed to dilution of HHCB and AHTN in water. In consequence, measured values would then be lower than those predicted by QWASI. In addition, effluents are recognized sources of suspended solids in streams (AECOM et al., 2011), which could adsorb musks and increase deposition in sediment, therefore removing musks dissolved in water.

In compartment D, HHCB and AHTN predicted values were higher than measured outflow concentrations, comparing 165 to 122 $ng \cdot L^{-1}$ (135%) and 7.03 to 5.46 $ng \cdot L^{-1}$ (129%), respectively (Figure 4.4). This may be due as well by interferences from tributaries. Two industrial effluents and one tributary, located one, two and three kilometers from GBWWTP are releasing water in compartment D from the North Saskatchewan River right bank (AECOM et al., 2011). The two industrial effluents, including the refinery discussed above, release respectively 262 and 18.8 $m^3 \cdot h^{-1}$. The volume contribution of the natural tributary is not reported. These localized inputs in the NSR, given the assumption they are musk free, are likely to favor dilution and mixing and lead to lower concentrations than those predicted in outflow water from compartment D i.e., at NSR5.

In compartment E, QWASI was able to explain better the fate of both musks with given environmental properties (Table 4.2). The model predicted 105% and 120% of HHCB and AHTN concentrations in water, respectively.

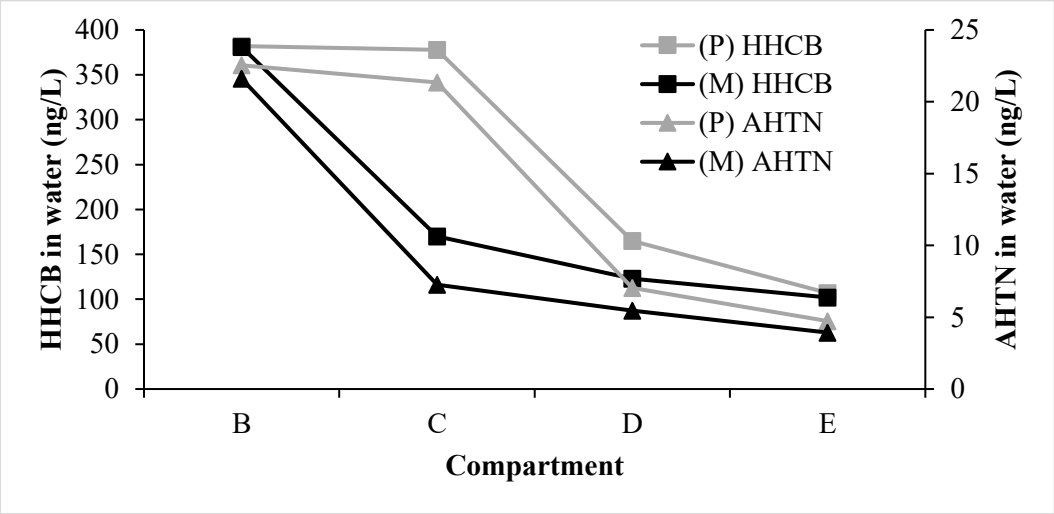

Figure 4.4. Predicted (P, grey) versus measured (M, black) musk concentrations ($ng \cdot L^{-1}$) in water from the North Saskatchewan River, Edmonton (AB, CAN) at outflow of compartments B, C, D and E, the respective cross-sections at sites NSR3, 4, 5 and 6. Predicted values were obtained with fate modelling using Quantitative Water Air Sediment Interaction model software.

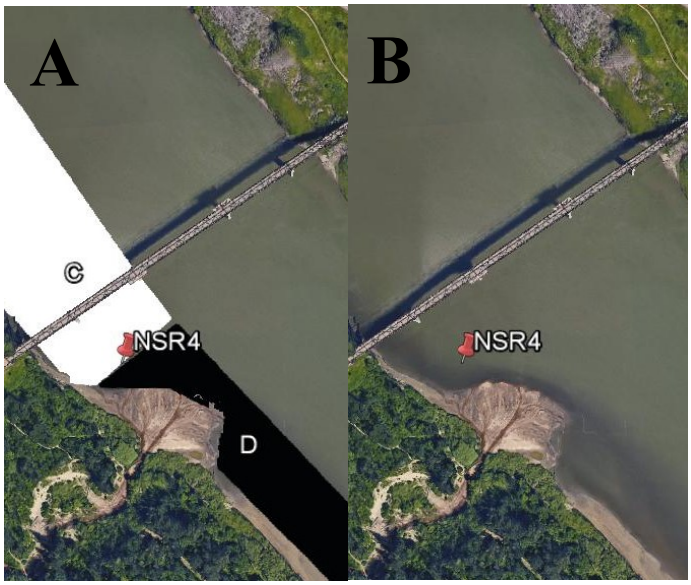

Figure 4.5. Imperial Oil Strathcona Refinery outfall (A) showing compartments C and D and (B) without compartments, on the right bank of the North Saskatchewan River, 1 km downstream of Gold Bar wastewater treatment plant in Edmonton (AB, CAN).

4.5. Conclusion

In this analysis, environmental inputs to QWASI were able to explain most of HHCB and AHTN fate in the North Saskatchewan River. The model generally slightly overestimated concentrations in the NSR with an expected error of on average 2.3% from measured results for compartment B and 22% for compartment D and E. The model failed to predict concentrations in compartment C, likely due to geographical environmental characteristics, i.e. the proximity of a refinery effluent. In order of importance, this analysis indicated that the fate of HHCB and AHTN in the North Saskatchewan was mostly driven by water outflow, sedimentation and water transformation. Predicted sediment concentrations were higher than comparable measurements from previous publications.

Chapter 5

General concluding remarks and future directions

The main objective of this thesis was to examine the behavior of two synthetic musks HHCB and AHTN in a contaminated urban waterbody by characterizing their levels in exposed fish, bioconcentration factors and contaminant fate near effluent outfalls. The development of an analytical method was a critical step in the realization of our goals and allowed us to determine concentrations of musks in fish exposed to fragrances *in vivo* as well as bioconcentration factors. The analytical method developed here for quantification of musks in fish will improve options available to scientists for reliable detection of musks in fish tissues. This work allowed to draw conclusions regarding analytical methods. The extraction of fresh fish samples with an in-cell sorbent such as alumina neutral was conducted in order to facilitate the purification of samples prior to gas-chromatography. That combination failed to remove lipids effectively from our fish extracts. Also, when working with d10-fluoranthene as a recovery standard, using Florisil for interferences removal in fish extracts may have induced variable recoveries possibly due to irreversible retention of PAHs.

Furthermore, the results presented in this thesis regarding the concentration of musks in exposed fish contributed to the growing and necessary evidence showing the persistence and bioaccumulative properties of two polycyclic musks. Concentrations of HHCB and AHTN in contaminated river water receiving wastewater effluent, as well as concentrations in exposed fathead minnows (FHMs), decreased significantly with distance from the source. Concentrations of HHCB in FHMs at the most contaminated sites were comparable to effect doses reducing vitellogenin in female rainbow trout (Simmons et al., 2010), but were lower than doses moderately decreasing the activity of two steroidogenic enzymes in male European sea bass (Fernandes et al., 2013). Bioconcentration factors of musks in fathead minnows were comparable or higher than those reported in the literature, and at most contaminated site, they were indicative of lower biotransformation rates.

Fugacity modeling with QWASI software allowed the description of the fate of HHCB and AHTN in the North Saskatchewan River (NSR), and the development of a modelling framework for predicting synthetic musks in an urban river. The fate of both musks were driven by the following processes, in order of importance: water outflow, sedimentation, reaction in water and volatilization. Predicted sediment concentrations were found to be higher than published measured data in effluent outfall sediment, which suggested that the half-life in sediment used for our predictions may not have been accurate. More research is suggested on the half-lives of musks in sediment. A comparison of predicted to measured concentrations of musks in water showed that fugacity modelling with QWASI version 3.00 (CEMC, 2005) succeeded in predicting concentrations in most compartments, and overestimated concentrations in water close to an outfall.

We hope the results of our work will solidify the basis on which decisions are made toward the regulation of synthetic fragrances in Canada and elsewhere. The next step to take in evaluating the impacts of HHCB and AHTN in aquatic ecosystems could be to assess the uptake and elimination dynamics in sensitive fish species exposed to different stress levels. As documented here, musks bioconcentrated to a larger extent in fish showing indications of oxidative stress (Jasinska et al.,2015) from the most contaminated sites. Oxidative stress can be caused by a variety of factors in aquatic ecosystems, and information is needed in order to confirm if stress affect musk accumulation and induce adverse effects on reproductive health in fish. In addition, scientific knowledge on synthetic musks could benefit from work on determination of half-lives of musks in fish as well as in sediments. Such work would allow a better understanding of the fate of these chemicals in water bodies. Musks are present in substantial quantities in urban area waterbodies and their potential for harm should not be overlooked, in male as much as in female fish. Work is still needed on the effects of long term exposure to synthetic musks *in vivo* at monitored concentrations in order to investigate their potential to cause harm on different generations of fish.

References

AECOM; Anderson, A. M. *Synthesis of recent knowledge on water quality, sediment quality and non-fish biota in the North Saskatchewan River, with special emphasis on the industrial heartland-capital region water management framework reach*; Alberta Environment: **2011**.

AIHA (Alberta Industrial Heartland Association). *Alberta's Industrial Heartland Association*. **2011**. (http://www.industrialheartland.com/).

An, J.; Zhou, Q.; Sun, Y.; Xu, Z., Ecotoxicological effects of typical personal care products on seed germination and seedling development of wheat (*Triticum aestivum L.*). *Chemosphere* **2009,** *76*, 1428-1434.

Aschmann, S. M.; Arey, J.; Atkinson, R.; Simonich, S. L., Atmospheric lifetimes and fates of selected fragrance materials and volatile model compounds. *Environ. Sci. Technol.* **2001,** *35*, 3595-3600.

Arnot, J. A.; Gobas, F. A. P. C., A review of bioconcentration factor (BCF) and bioaccumulation factor (BAF) assessments for organic chemicals in aquatic organisms. *Env. Rev.* **2006,** *14*, 257-297.

Artola-Garicano, E.; Sinnige, T. L.; Holsteijn, I. V.; Vaes, W. H. J.; Hermens, J. L. M., Bioconcentration and acute toxicity of polycyclic musks in two benthic organisms (*Chironomus riparius* and *Lumbriculus variegatus*). *Environmental Toxicology and Chemistry* **2003,** *22*, (5), 1086-1092.

Balk, F.; Ford, R. A., Environmental risk assessment for the polycyclic musks AHTN and HHCB in the EU. Part I. Fate and exposure assessment. *Toxicology Letters* **1999a,** *111*, 57-79.

Balk, F.; Ford, R. A., Environmental risk assessment for the polycyclic musks, AHTN and HHCB II. Effect assessment and risk characterization. *Toxicology Letters* **1999,** *111*, 81-94.

Bester, K., Polycyclic musks in the Ruhr catchment area—transport, discharges of wastewater, and transformations of HHCB, AHTN and HHCB-lactone. *J. Environ. Monit.* **2005,** *7*, 43-51.

Bester, K., Analysis of musk fragrances in environmental samples. *Journal of Chromatography A* **2009,** *1216*, 470-480.

Boethling, R. S., Incorporating environmental attributes into musk design. *Green Chem.* **2011,** *13*, 3386-3396.

Buczynska, A. J.; Geypens, B.; Grieken, R.; De Wael, K., Optimization of sample clean-up for the GC-C-IRMS and GC-IT-MS analyses of PAHs from air particulate matter. *Microchemical Journal*, **2015**, (119), 83-92.

Buerge, I. J.; Buser, H.-R.; Muller, M. D.; Poiger, T., Behavior of the polycyclic musks HHCB and AHTN in lakes, two potential anthropogenic markers for domestic wastewater in surface waters. *Environ. Sci. Technol.* **2003,** *37*, 5636-5644.

CEMC (Canadian environmental modelling center, Trent University), QWASI (Quantitative Water Air Sediment Interaction) model software, version 3.00, **2005.** *Based on Mackay, D., Multimedia Environmental Models: The Fugacity Approach - Second Edition, Lewis publishers, Boca Raton,* ***2001,*** *201-213.*

Chen, C.; Zhou, Q.; Liu, S.; Xiu, Z., Acute toxicity, biochemical and gene expression responses of the earthworm *Eisenia fetida* exposed to polycyclic musks. *Chemosphere* **2011,** *83*, 1147-1154.

Chen, C.; Zhou, Q.; Cai, Z., Effect of soil HHCB on cadmium accumulation and phytotoxicity in wheat seedlings. *Ecotoxicology* **2014,** *23*, 1996-2004.

Chen, F.; Ying, G.-G.; Ma, Y.-B.; Chen, Z.-F.; Lai, H.-J., Field dissipation of four personal care products in biosolids-amended soils in North China. *Environmental Toxicology and Chemistry* **2014,** *33*, (11), 2413-2421.

Chen, F.; Gao, J.; Zhou, Q., Toxicity assessment of simulated urban runoff containing polycyclic musks and cadmium in *Carassius auratus* using oxidative stress biomarkers. *Environmental Pollution* **2012,** *162*, 91-97.

Chen, X.; Pauly, U.; Rehfus, S.; Bester, K., Personal care compounds in a reed bed sludge treatment system. *Chemosphere* **2009,** *76*, 1094-1101.

Clara, M.; Gans, O.; Windhofer, G.; Krenn, U.; Hartl, W.; Braun, K.; Scharf, S.; Sheffknecht, C., Occurence of polycyclic musks in wastewater and receiving water bodies and fate during wastewater treatment. *Chemosphere* **2011,** *82*, 1116-1123.

COE (City of Edmonton), Historical Loading to the North Saskatchewan River from Edmonton (1878 – 2009). Drainage Information Systems, Drainage Services, City of Edmonton. October 2010.

Davis, D. A.; Taylor, J. M.; Jones, W. I.; Brouwer, J. B., Toxicity of musk ambrette. *Toxicology and Applied Pharmacology* **1967,** *10*, (2), 405.

Del Rio, H.; Suarez, J.; Puertas, J.; Ures, P., PPCPs wet weather mobilization in a combined sewer in NW Spain. *Science of the Total Environment* **2013,** *449*, 189-198.

Draisci, R.; Marchiafava, C.; Ferretti, E.; Palleschi, L.; Catellani, G.; Anastasio, A., Evaluation of musk contamination of freshwater fish in Italy by accelerated solvent extraction and gas chromatography with mass spectrometric detection. *Journal of Chromatography A*, **1998**, (814), 187-197.

ECHA, European Chemical Agency, *Candidate list of substances of very high concern for authorisation*. **2015**. (http://echa.europa.eu/web/guest/candidate-list-table)

Envirogen, *Fate of HHCB in soil microcosms*; Princeton Research Centre, NJ: Union Beach, NJ, USA, 1998.

EPA, Environmental Protection Agency of the United States, *Semivolatile organic compounds*. **2015**. (http://www.epa.gov/reg3hwmd/bf-lr/regional/analytical/semi-volatile.htm)

EPCOR, Edmonton Power Corporation, *Gold Bar wastewater treatment plant*. **2015**. (http://corp.epcor.com/watersolutions/operations/edmonton/goldbar/pages/gold-bar-wastewater-treatment-plant.aspx)

Fernandes, D.; Dimastrogiovanni, G.; Blázquez, M.; Porte, C., Metabolism of the polycyclic musk Galaxolide and its interference with endogenous and xenobiotic metabolizing enzymes in the European sea bass (*Dicentrarchus labrax*). *Environmental Pollution* **2013,** *174*, 214-221.

Franke, S.; Meyer, C.; Heinzel, N.; Gatermann, R.; Hühnerfuss, H.; Rimkus, G.; König, W. A.; Francke, W., Enantiomeric composition of the polycyclic musks HHCB and AHTN in different aquatic species. *Chirality* **1999,** *11*, 795-801.

Frater, G.; Müller, U.; Kraft, P., Preparation and olfactory characterization of the enantiomerically pure isomers of the perfumery synthetic Galaxolide. *Helvetica Chimica Acta* **1999,** *82*, 1656-1665.

Fromme, H.; Otto, T.; Pilz, K.; Neugebauer, F., Levels of synthetic musks; bromocyclene and PCBs in eel (*Anguilla Anguilla*) and PCBs in sediments samples from some waters of Berlin/Germany. *Chemosphere* **1999,** *39*, (10), 1723-1735.

Fromme, H.; Lahrz, T.; Piloty, M.; Gebhart, H.; Oddoy, A.; Rüden, H., Occurrence of phthalates and musk fragrances in indoor air and dust from apartments and kindergartens in Berlin (Germany). *Indoor Air* **2004,** *14*, (3), 188-195.

Gatermann, R.; Biselli, S.; Hühnerfuss, H.; Rimkus, G. G.; Hecker, M.; Karbe, L., Synthetic musks in the environment. Part 1: Species-dependent bioaccumulation of polycyclic and nitro musk fragrances in freshwater fish and mussels. *Arch. Environ. Contam. Toxicol.* **2002,** *42*, 437-446.

Gatermann, R.; Biselli, S.; Hühnerfuss, H.; Rimkus, G. G.; Franke, S.; Hecker, M.; Kallenborn, R.; Karbe, L.; König, W. A., Synthetic musks in the environment. Part 2: Enantioselective transformation of the polycyclic musk fragrances HHCB, AHTN, AHDI, and ATII in freshwater fish. *Arch. Environ. Contam. Toxicol.* **2002,** *42*, 447-453.

Government of Canada, *Climate: Monthly Data Report for 2011*. **2015**. (http://climate.weather.gc.ca/climateData/monthlydata_e.html?timeframe=3&Prov=AB&StationID=1865&mlyRange=1959-01-01|2012-04-01&Year=2011&Month=1&Day=1)

Heberer, T., Occurrence, fate, and assessment of polycyclic musk residues in the aquatic environment of urban areas – a review. *Acta hydrochim. hydrobiol.* **2002,** *30*, (5-6), 227-243.

Helm, P. A.; Howell, E. T.; Li, H.; Metcalfe, T. L.; Chomicki, K. M.; Metcalfe, C. D., Influence of the nearshore dynamics on the distribution of organic wastewater-associated chemicals in Lake Ontario determined using passive samplers. *Journal of Great Lakes Research* **2012,** *38*, (4), 105-115.

HERA *Polycyclic musks AHTN (CAS 1506-02-1) and HHCB (CAS 1222-05-5), environmental section*; Human and Environmental Risk Assessment on Ingredients of Household Cleaning Products: 2004; p 81

Hu, Z.; Shi, Y.; Niu, H.; Cai, Y.; Jiang, G.; Wu, Y., Occurrence of synthetic musk fragrances in human blood from 11 cities in China. *Environmental Toxicology and Chemistry* **2009,** *29*, 1877-1882.

Hu, Z.; Shi, Y.; Cai, Y., Reprint of: Concentrations, distribution, and bioaccumulation of synthetic musks in the Haihe River of China. *Chemosphere* **2011,** *85*, 262-267.

Janzen, N.; Dopp, E.; Hesse, J.; Richards, J.; Türk, J.; Bester, K., Transformation products and reaction kinetics of fragrances in advanced wastewater treatment with ozone. *Chemosphere* **2011,** *85*, 1481-1486.

Jasinska, E. J.; Goss, G. G.; Gillis, P. L.; Kraak, G. J. V. D.; Matsumoto, J.; Machado, A. A. d. S.; Giacomin, M.; Moon, T. W.; Massarsky, A.; Gagné, F.; Servos, M. R.; Wilson, J.; Sultana, T.; Metcalfe, C. D., Assessment of biomarkers for contaminants of emerging concern on aquatic organisms dowstream of a municipal wastewater discharge. *Science of the Total Environment* **2015,** *530-531*, 140-153.

Kannan, K.; Reiner, J. L.; Yun, S. H.; Perrotta, E. E.; Tao, L.; Johnson-Restrepo, B.; Rodan, B. D., Polycyclic musk compounds in higher trophic level aquatic organisms and humans from the United States. *Chemosphere* **2005,** *61*, 693-700.

Kidd, K. A.; Paterson, M. J.; Rennie, M. D.; Podemski, C. L.; Findlay, D. L.; Blanchfield, P. J.; Liber, K., Direct and indirect responses of a freshwater food web to a potent synthetic oestrogen. *Phil. Trans. R. Soc. B* **2014**, *369*, 1-11

Klaschka, U.; Carsten von der Ohe, P.; Bschorer, A.; Krezmer, S.; Sengl, M.; Letzel, M., Occurences and potential risks of 16 fragrances in five German sewage treatment plants and their receiving waters. *Environ Sci Pollut Res* **2013,** *20*, 2456-2471.

Köster, D.; Gregor, D.; Geiger, C.; Forrest, F.; Hutchinson, N. J. *North Saskatchewan River: Water quality and related studies (2007-2012)*; Alberta Environment and Sustainable Resource Development: Edmonton, **2014**.

LAERD Statistics, One-way ANOVA. **2016**. (https://statistics.laerd.com/statistical-guides/one-way-anova-statistical-guide-3.php)

Langworthy DE, NR Itrich, SL Simonich, TW Federle. Biotransformation of the polycyclic musk, HHCB, in activated sludge and river water. Poster presented at SETAC World Congress, Brighton, UK, May **2000**.

Lu, Y.; Yuan, T.; Wang, W.; Kannan, K., Concentrations and assessment of exposure to siloxanes and synthetic musks in personal care products from China. *Environmental Pollution* **2011,** *159*, 3522-3528.

Luckenbach, T.; Corsi, I.; Epel, D., Fatal attraction: Synthetic musk fragrances compromise multixenobiotic defense systems in mussels. *Marine Environmental Research* **2004,** *58*, 215-219.

Lung, S.-C. C.; Liu, C.-H., High-sensitivity analysis of six synthetic musks by ultra-performance liquid chromatography-atmospheric pressure photoionization-tandem mass spectrometry. *Analytical Chemistry* **2011,** *83*, 4955-4961.

Mackay, D.; Paterson, S.; Joy, M., A quantitative water, air, sediment interaction (QWASI) fugacity model for describing the fate of chemicals in rivers. *Chemosphere* **1983,** *12*, (9/10), 1193-1208.

Mackay, D., *Multimedia environmental models: The fugacity approach*. United-States, **1991**.

Maekawa, A.; Matsushima, Y.; Onodera, H.; Shibutani, M.; Ogasawara, H.; Kodama, Y.; Kurokawa, Y.; Hayashi, Y., Long-term toxicity/carcinogenicity of musk xylol in B6B3F mice. *Food and Chemical Toxicology* **1990,** *28*, (8), 581-586.

Martinez, E.; Gros, M.; Lacorte, S.; Barcelò, D., Simplified procedures for the analysis of polycyclic aromatic hydrocarbons in water, sediments and mussels. *Journal of Chromatography A*, **2004**, (1047), 181-188.

Melymuk, L.; Robson, M.; Csiszar, S. A.; Helm, P. A.; Kaltenecker, G.; Backus, S.; Bradley, L.; Gilbert, B.; Blanchard, P., Jantunen, L.; Diamond, M. L., From the city to the lake: loadings of PCBs, PBDEs, PAHs, and PCMs from Toronto to Lake Ontario. *Environ. Sci. Technol*. **2014**, *48*, 3732-3741

Mori, T.; Morita, F.; Inokuchi, A.; Takao, Y.; Kohra, S.; Tominaga, N.; Takemasa, T.; Arizono, K., Ecotoxicological effect of polycyclic musks on *Caenorhabditis elegans*. *Journal of Health Science* **2006,** *52*, (3), 276-282.

Mottaleb, A.M.; Osemwengie, L.I.; Islam, R. M.; Sovocool, W. G., Identification of bound nitro musk-protein adducts in fish liver by gas chromatography–mass spectrometry: Biotransformation, dose–response and toxicokinetics of nitro musk metabolites protein adducts in trout liver as biomarkers of exposure. *Aquatic Toxicology*, **2012**, 164-172.

OSPAR comission, *Musk xylene and other musks*; 2004

O'Toole, S.; Metcalfe, C., Synthetic musks in fish from urbanized areas of the lower Great Lakes, Canada. *J. Great Lakes Res.* **2006,** *32*, 361-369.

Peck, A. M.; Hornbuckle, K. C., Synthetic musk fragrances in Lake Michigan. *Environ. Sci. Technol.* **2004,** *38*, 367-372.

Peck, A. M.; Hornbuckle, K. C., Synthetic musk fragrances in urban and rural air of Iowa and the Great Lakes. *Atmospheric Environment* **2006,** *40*, (32), 6101-6111.

Peck, A. M.; Kucklick, J. R.; Schantz, M. M., Synthetic musk fragrances in environmental Standard Reference Materials. *Anal Bioanal Chem* **2007,** *387*, 2381-2388.

Pilechi, A.; Rennie, C. D.; Mohammadian, M.; Zhu, D.; Delatolla, R. *Physical mixing patterns of water and contaminants in the North Saskatchewan River*; Alberta Environment, **2012**.

Ricking, M.; Schwarzbauer, J.; Hellou, J.; Svenson, A.; Zitko, V., Polycyclic aromatic musk compounds in sewage treatment plant effluents of Canada and Sweden - firsts results. *Marine Pollution Bulletin* **2003,** *46*, 410-417.

Rimkus, G.; Rimkus, B.; Wolf, M., Nitro musks in human adipose tissue and breast milk. *Chemosphere* **1994,** *28*, (2), 421-432.

Rowe, D. J., *Chemistry and technology of flavors and fragrances*. USA and Canada, **2005**; p 336

Rüdel, H.; Böhmer, W.; Schröter-Kermani, C., Retrospective monitoring of synthetic musk compounds in aquatic biota from German rivers and coastal areas. *Journal of Environmental Monitoring* **2006,** *8*, 812-823.

Santiago-Morales, J.; Gomez, M. J.; Herrera-Lopez, S.; Fernandez-Alba, A. R.; Garcia-Calvo, E.; Rosal, R., Energy efficiency for the removal of non-polar pollutants during ultraviolet irradiation, visible light photocatalysis and ozonation of a wastewater effluent. *Water Research* **2013,** *47*, 5546-5556.

Schnell, S.; Martin-Skilton, R.; Fernandes, D.; Porte, C., The interference of nitro- and polycyclic musks with endogenous and xenobiotic metabolizing enzymes in carp: an in vitro study. . *Environmental Science Technology* **2009,** *43*, 9458-9464.

Schreurs, R. H. M. M.; Quaedackers, M. E.; Seinen, W.; Van der Burg, B., Transcriptional activation of estrogen receptor ERa and ERb by polycyclic musks is cell type dependant. *Toxicology and Applied Pharmacology* **2002,** *183*, 1-9.

Schreurs, R. H. M. M.; Sonneveld, E.; Jansen, J. H. J.; Seinen, W.; Van der Burg, B., Interaction of polycyclic musks and UV filters with the estrogen receptor (ER), androgen receptor (AR), and progesterone receptor (PR) in reporter gene bioassays. *Toxicological sciences* **2005,** *83*, 264-272.

Shek, W. M.; Murphy, M. B.; Lam, J. C. W.; Lam, P. K. S., Synthetic polycyclic musks in Hong Kong sewage sludge. *Chemosphere* **2008,** *71*, 1241-1250.

Simmons, D. B. D.; Marlatt, V. L.; Trudeau, V. L.; Sherry, J. P.; Metcalfe, C. D., Interaction of Galaxolide® with the human and trout estrogen receptor-α. *Science of the Total Environment* **2010,** *408*, 6158-6164.

Spencer, P. S.; Bischoff-Fenton, M. C.; Moreno, O. M.; Donald L. Opdyke; Ford, R. A., Neurotoxic properties of musk ambrette. *Toxicology and Applied Pharmacology* **1984,** *75*, (3), 571-575.

Stantec, *Setting gold standard - Gold Bar wastewater treatment plant, Edmonton, Alberta*. **2015**.

(http://www.stantec.com/our-work/projects/canada-projects/g/gold-bar-wastewater-treatment-plant.html#.Vb40Sm5Viko)

Statistics Canada. 2012. *Focus on Geography Series, 2011 Census*. Statistics Canada Catalogue no. 98-310-XWE2011004. Ottawa, Ontario. Analytical products, **2011** Census. Last updated October 24, 2012.

Stockholm Convention. *Listing of POPs in the Stockholm Convention*. **2008** http://chm.pops.int/Convention/ThePOPs/ListingofPOPs/tabid/2509/Default.aspx

Sumner, N. R.; Guitart, C.; Fuentes, G.; Readman, J. W., Inputs and distributions of synthetic musk fragrances in an estuarine and coastal environment; a case study. *Environmental Pollution* **2010,** *158*, 215-222.

Weschler, C. J.; Nazaroff, W. W., Semivolatile organic compounds in indoor environments. *Atmospheric Environment* **2008,** *42*, 9018-9040.

Valdersnes, S.; Kallenborn, R.; Sydnes, L. K., Identification of several Tonalide transformation products in the environment. *Intern. J. Environ. Anal. Chem.* **2006,** *86*, (7), 461-471.

Van der Burg, B.; Schreurs, R.; Linden, S. v. d.; Seinen, W.; Brouwer, A.; Soneveld, E., Endocrine effects of polycyclic musks: do we smell a rat? *International journal of andrology* **2008,** *31*, 188-193.

Wollenberger; Breitholtz, M.; Kusk, K. O.; Bengtsson, B.-E., Inhibition of larval development of the marine copepod *Acartia tonsa* by four synthetic musk substances. *The Science of the Total Environment* **2003,** *305*, 53-64.

Yamauchi, R.; Ishibashi, H.; Hirano, M.; Mori, T.; Kim, J.-W.; Arizono, K., Effects of synthetic polycyclic musks on estrogen receptor, vitellogenin, pregnane X receptor, and cytochrome P450 3A gene expression in the livers of male medaka (*Oryzias latipes*). *Aquatic Toxicology* **2008,** *90*, 261-268.

Zhang, X.; Yao, Y.; Zeng, X.; Qian, G.; Guo, Y.; Wu, M.; Sheng, G.; Fu, J., Synthetic musks in the aquatic environment and personal care products in Shanghai, China. *Chemosphere* **2008,** *72*, 1553-1558.

Zhang, L.; An, J.; Zhou, Q., Single and joint effects of HHCB and cadmium on zebrafish (*Danio rerio*) in feculent water containing bedloads. *Front. Environ. Sci. Eng.* **2012,** *6*, (3), 360-372.

Zhang, X.; Xu, Q.; Man, S.; Zeng, X.; Yu, Y.; Pang, Y.; Sheng, G.; Fu, J., Tissue concentrations, bioaccumulation, and biomagnification of synthetic musks in freshwater fish from Taihu Lake, China. *Environ Sci Pollut Res* **2013,** *20*, 311-322.

Appendix

Appendix A

List of presentations

Oral presentations

Claudine Lefebvre, Linda Kimpe, Chris Metcalfe, Vance Trudeau, Jules Blais. Quantification of Polycyclic Musks HHCB and AHTN in Fathead Minnows from Edmonton, North Saskatchewan River, around Gold Bar Wastewater Treatment Plant. 41st Aquatic Toxicity Workshop, Ottawa, Ontario, September 29- October 1rst, 2014

Claudine Lefebvre, Linda Kimpe, Chris Metcalfe, Vance Trudeau, Jules Blais. Quantification of Polycyclic Musks HHCB and AHTN in Fathead Minnows from Edmonton, North Saskatchewan River, around Gold Bar Wastewater Treatment Plant. Genomes to Biomes and Canadian Society for Ecology and Evolution, Society of Canadian Limnologists and Canadian Society of Zoologists, Montreal, Quebec, May 25-29, 2014.

Poster presentations

Claudine Lefebvre, Linda Kimpe, Chris Metcalfe, Vance Trudeau, Jules Blais. Fragrant fish: Presence and bioconcentration potential of polycyclic musks Galaxolide and Tonalide in fathead minnows (*Pimephales promelas*) from North Saskatchewan River, Edmonton. Canadian Conference for Fisheries Research and Society of Canadian Limnologists, Ottawa, Ontario, January 8-11, 2015.

Appendix B

Musk ratios in fathead minnows

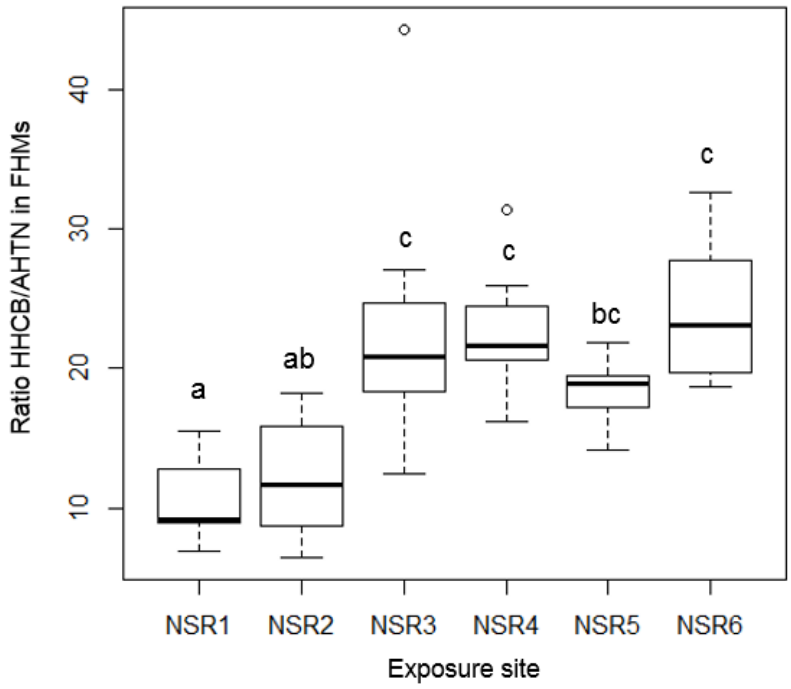

Figure B1. Distribution the ratios of HHCB to AHTN concentrations (no units) in exposed fathead minnows. Boxes show from top to bottom the upper quartile, median and lower quartile. The whiskers show the maximum and minimum values excluding outliers, the latter represented by the hollow points. The letters a, b and c acknowledge for statistical differences between groups tested in a one-way ANOVA. For NSR1 and NSR4, n=10, for NSR2, NSR3 and NSR6, n= 12 and for NSR5, n=11.

Appendix C

Fugacity model: compartments division

Table C1. Compartment widths at several cross sections of the North Saskatchewan River in accordance with the mixing of the Gold Bar effluent (Edmonton, AB, CAN) (Pilechi et al., 2012). The negative cross sections were located upstream of Gold Bar. The widths were based from the right bank (or South bank) of the river due to the effluent being released from that side. Mixing information was available at distances identified with an asterix.

Distance from Gold Bar	Compartment	Width from right bank	Total cross section length	% of cross section
km		m	m	
-1.074	A	186	186	100
-0.009	A	167	167	100
-0.009	B	47	167	28
0.094*	B	49	166	30
0.181	B-C	61	178	34
0.595	C	64	196	33
1.096	C	76	213	36
1.114	C-D	76	210	36
1.598	D	67	174	39
2.101	D	53	138	38
2.599	D	63	168	38
3.104	D	75	183	41
3.604	D	94	225	42
3.747	D-E	95	223	43
4.105	E	97	208	47
4.606	E	100	211	47
5.111	E	105	219	48
5.613	E	115	225	51
6.116	E	91	171	53
6.616	E	84	150	56
7.117	E	142	248	57
7.621	E	125	214	58
8.126	E	124	207	60
8.631	E	132	211	63
9.130	E	141	221	64
9.526*	E	150	219	65
9.997	E-F	166	224	74
10.497	F	191	237	81
10.997	F	216	236	92
11.644*	F	203	203	100

Appendix D

Reported musk ratios (HHCB to AHTN)

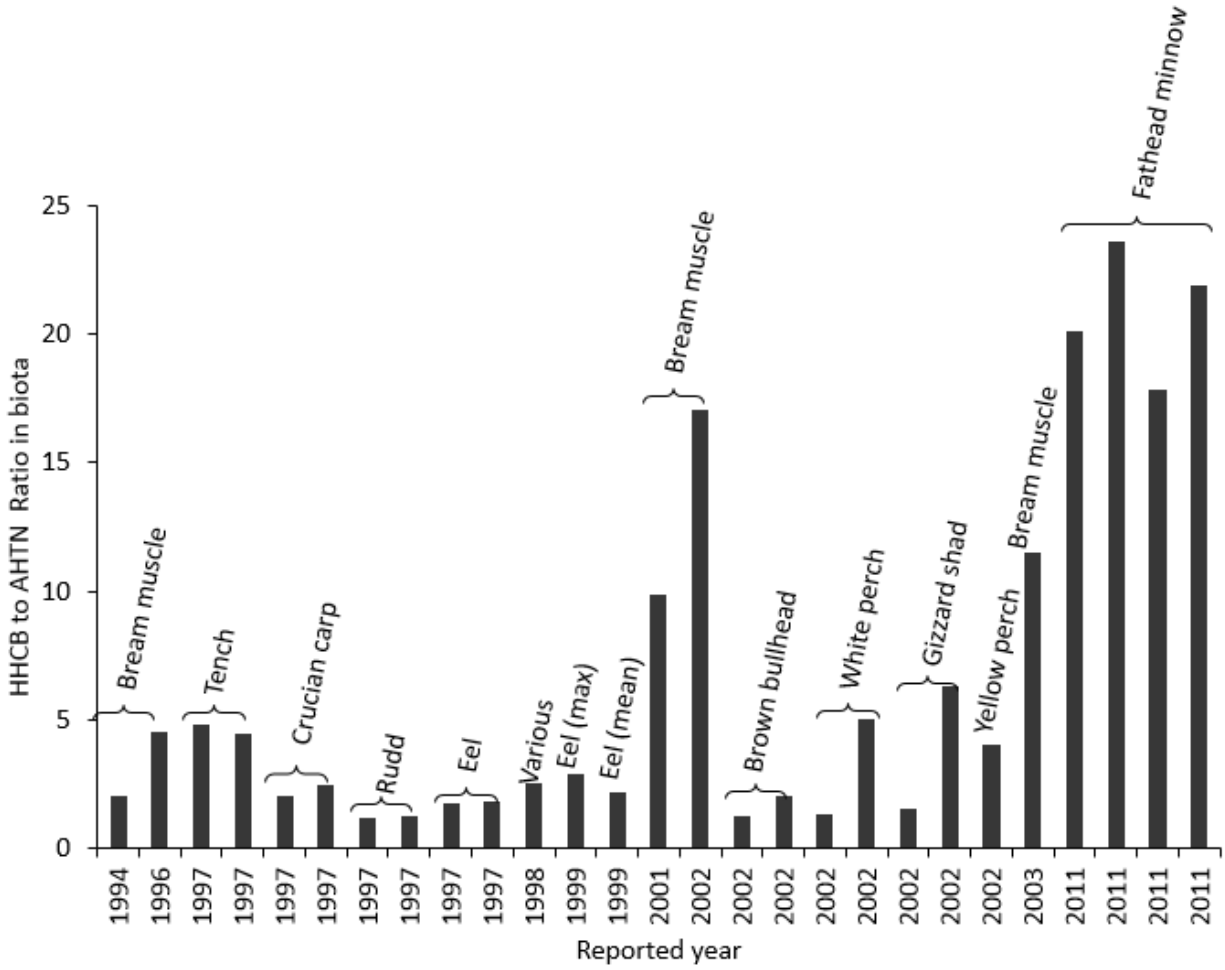

Figure D1. HHCB to AHTN ratios calculated with wet weight concentrations reported in biota sampled at various locations, from 1994 to 2011. Bream muscle (all years): Rüdel et al., 2006; Tench, Crucian carp, Rudd and Eel (1997): Gatermann et al., 2002 and Franke et al., 1999; Various species (1998): Heberer, 2002; Eel (1999): Fromme et al., 1999; Brown bullhead, White perch, Gizzard shad and Yellow perch (2002): O'Toole et al., 2006; Fathead minnows (2011): this project.